

# Crystallographic Investigation of Substituted Allyl and Titanacyclobutane Complexes of Bis(2-*N,N*-dialkylaminoindenyl)titanium. Structure and Reactivity as a Function of the Dialkylamino Substituents

Grace Greidanus, Robert McDonald,<sup>†</sup> and Jeffrey M. Stryker\*

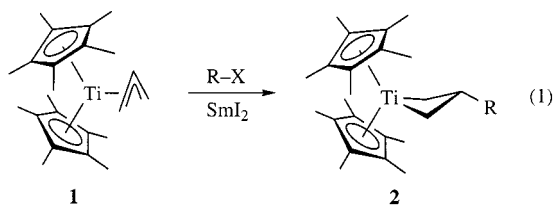
Department of Chemistry, University of Alberta, Edmonton, Alberta, T6G 2G2 Canada

Received September 18, 2000

Substituted allyl complexes of bis(2-*N,N*-dialkylaminoindenyl)titanium(III) undergo highly regioselective central carbon alkylation upon treatment with organic free radicals, providing a general synthesis of 2,3-disubstituted titanacyclobutane complexes. This reactivity contrasts that of the corresponding bis(pentamethylcyclopentadienyl)titanium(III) series, for which titanacyclobutane formation is observed only in reactions of the unsubstituted allyl complex. Unexpectedly, the radical alkylation is more general for complexes of bis(2-*N,N*-dimethylaminoindenyl)titanium than complexes of the closely analogous bis(2-piperidinoindenyl)titanium, despite only subtle differences between the two ancillary ligands. In addition, the 2-methyl-3-alkyltitanacyclobutane complexes derived from alkylation of bis(2-*N,N*-dimethylaminoindenyl)titanium( $\eta^3$ -crotyl) are more thermally robust than those derived from the 2-piperidinoindenyl ligand system, resisting decomposition via  $\beta$ -hydride elimination from the  $\alpha$ -methyl substituent. To gain insight into the function of the dialkylaminoindenyl ligands and to probe the differences between 2-*N,N*-dimethylaminoindenyl and 2-piperidinoindenyl complexes, crystal structures of bis(2-*N,N*-dimethylaminoindenyl)titanium( $\eta^3$ -1-phenylallyl) (**4a**) and bis(2-*N,N*-dimethylaminoindenyl)titanium( $\eta^3$ -crotyl) (**4b**) have been determined and compared to the crystal structure of bis(2-piperidinoindenyl)titanium( $\eta^3$ -1-phenylallyl), **3a**. The effects of allyl coordination on the disposition of the dialkylaminoindenyl ligands are revealed by a comparison with the crystal structure of the corresponding chloride complex, bis(2-*N,N*-dimethylaminoindenyl)titanium(III)chloride·lithium chloride·(THF)<sub>2</sub>, a rare Ti(III)halide/lithium halide adduct. Although it is difficult to control for the effects of crystal packing forces, substantial changes in ancillary ligand structure and orientation are observed as a function of the amino substituent and the coordination environment. The difference in titanacyclobutane stability and the response of the dialkylaminoindenyl ligands to the change in oxidation state have been investigated by comparing the crystal structures of two disubstituted titanacyclobutane complexes, 3-isopropyl-2-phenylbis(2-piperidinoindenyl)titanacyclobutane (**7**) and 3-isopropyl-2-phenylbis(2-*N,N*-dimethylaminoindenyl)titanacyclobutane (**8**), each prepared by free radical alkylation.

## Introduction

Permethyltitanocene(III)  $\eta^3$ -allyl complexes **1** undergo regioselective central carbon alkylation upon treatment with organic free radicals, yielding titanacyclobutane complexes **2** (eq 1).<sup>1</sup> Subsequent conversions to cyclic



organic compounds by isonitrile insertion<sup>2</sup> and carbo-

nylation<sup>3</sup> demonstrate the potential for substantive applications to organic synthesis. Based upon frontier molecular orbital analysis,<sup>4</sup> the regioselective radical alkylation should be particularly facile in pseudotetrahedral  $d^1$ -transition metal systems with significant  $d \rightarrow \pi^*$  back-bonding. This is supported by our observation that the relatively less electron rich complex  $Cp_2Ti(\eta^3\text{-allyl})$  generally fails to undergo central carbon alkylation.<sup>5</sup> Increasing the electron density at the metal center by using more electron rich ancillary ligands activates the system toward radical alkylation: allyl complexes

(1) (a) Casty, G. L.; Stryker, J. M. *J. Am. Chem. Soc.* **1995**, *117*, 7814. (b) Ogoshi, S.; Stryker, J. M. *J. Am. Chem. Soc.* **1998**, *120*, 3514.

(2) Carter, C. A. G.; Greidanus, G.; Stryker, J. M. Manuscript in preparation.

(3) Carter, C. A. G.; Greidanus, G.; Chen, J.-X.; Stryker, J. M. Manuscript submitted for publication.

(4) (a) Curtis, M. D.; Eisenstein, O. *Organometallics* **1984**, *3*, 887.

(b) Lauher, J. W.; Hoffman, R. *J. Am. Chem. Soc.* **1976**, *98*, 1729. (c) Green, J. C. *Chem. Soc. Rev.* **1998**, *27*, 263.

(5) Casty, G. L. Ph.D. Dissertation, Indiana University, 1994.

\* Corresponding author. Tel: (780) 492-3891. Fax: (780) 492-8231. E-mail: jeff.stryker@ualberta.ca.

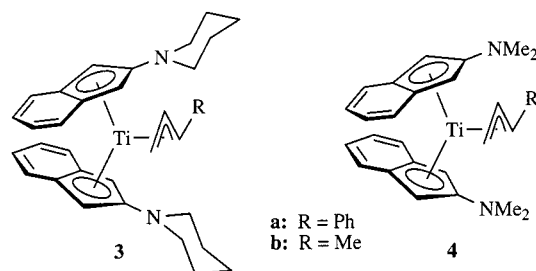
<sup>†</sup> Faculty Service Officer, Department of Chemistry Structure Determination Laboratory.

of both bis(*tert*-butylcyclopentadienyl)titanium and (cyclopentadienyl)(pentamethylcyclopentadienyl)titanium(III) react with organic radicals to produce titanacyclobutane complexes.<sup>5,6</sup>

None of these titanocene systems, however, tolerate substitution on the allyl ligand. Instead, radical addition presumably occurs at the metal center rather than at the central carbon of the allyl ligand.<sup>5-7</sup> The reason for this change in reactivity is not well understood; little information is available regarding the solution structure and dynamics of d<sup>1</sup>-metallocene allyl complexes.<sup>8</sup> However, a hapticity change from  $\eta^3$ - to  $\eta^1$ -coordination is often observed upon incorporation of allyl substituents in d<sup>0</sup>-metallocene complexes.<sup>9</sup> It is reasonable to propose that substituents on the allyl ligand also significantly influence the equilibrium between  $\eta^3$ - and  $\eta^1$ -coordination modes in d<sup>1</sup>-metallocene systems, particularly in donor solvents such as tetrahydrofuran. The  $\eta^1$ -coordination mode clearly disrupts the one-electron  $d(3a_1) \rightarrow \pi^*$  allyl back-bond<sup>1,4</sup> thought to be responsible for controlling the regioselectivity of  $\eta^3$ -allyl radical alkylation. Preferential  $\eta^1$ -allyl coordination in substituted permethyltitanocene(III) allyl complexes might arise from a confluence of unfavorable steric interactions between the allyl and ancillary ligands and the inherently weaker metal-carbon bonding anticipated at the substituted position. Unfortunately, less sterically demanding systems such as bis(*tert*-butylcyclopentadienyl)titanium,<sup>5</sup> (cyclopentadienyl)(pentamethylcyclopentadienyl)titanium,<sup>6</sup> and bis(trimethylsilylcyclopentadienyl)titanium<sup>7</sup> also fail to undergo radical alkylation at the central carbon of substituted allyl ligands.

Given this analysis, we anticipated that strongly electron donating dialkylamino-substituted titanocene templates would promote selective central carbon alkylation at substituted allyl ligands by enhancing the one-electron  $d(3a_1) \rightarrow \pi^*$  back-bond without imposing steric interactions unfavorable to  $\eta^3$ -coordination. Thus, we recently reported the radical alkylation of substituted allyl complexes by using the bis(2-piperidinoindenyl)titanium(III) template **3**, providing a stereoselective synthesis of 2,3-disubstituted titanacyclobutane complexes.<sup>10</sup> The success of the 2-piperidinoindenyl template, however, appears to be limited to alkylation by

unstabilized alkyl radicals. More importantly, disubstituted titanacyclobutane complexes derived from radical alkylation of 1-methylallyl (crotyl) complexes proved to be thermally sensitive, degrading rapidly in solution via  $\beta$ -hydride elimination from the  $\alpha$ -methyl substituent.<sup>7,10</sup> Unfavorable steric interactions generated by the relatively large piperidino substituents on the indenyl rings were proposed to be at least partly responsible for the relative facility of this  $\beta$ -hydride elimination.



For these reasons, the development of the less sterically demanding but similarly electron-rich bis(2-*N,N*-dimethylaminoindenyl)titanium(III) template **4** was initiated. Despite this apparently subtle change in structure, the 2-*N,N*-dimethylaminoindenyl system is compatible with an extended range of radical alkylations<sup>11</sup> and, as reported here, dramatically increases the thermal stability of the resultant  $\alpha$ -methyl-substituted titanacyclobutane complexes. To gain insight into the use of dialkylaminoindenyl ligands to promote central carbon alkylation of substituted allyl complexes and to probe differences between the piperidino- and dimethylamino-substituted indenyl ligands, we have undertaken a comparative crystallographic investigation of both substituted titanium(III) allyl complexes and derived titana(IV)cyclobutane complexes for each of the two amino-substituted indenyl ligand systems.

## Experimental Section

**General Procedures.** Air-sensitive manipulations were performed under a nitrogen atmosphere using standard Schlenk techniques or in a nitrogen-filled drybox. Solvents were purified by distillation from sodium or potassium benzophenone ketyl. Infrared (IR) spectra were obtained using compounds applied as a film to KBr or KCl salt plates ("casts") and are reported in wavenumbers ( $\text{cm}^{-1}$ ) calibrated to the 1601  $\text{cm}^{-1}$  absorption of polystyrene. HMQC NMR spectroscopic experiments are inverse-detection heterocorrelated ( $^1\text{H}/^{13}\text{C}$ ) spectra recorded at the  $^1\text{H}$  frequency of the spectrometer. Chemical shifts are reported in the  $\delta$  scale, referenced to residual protiated solvent. High-resolution mass spectra were obtained in electron impact mode operating at 40 eV. Combustion analyses were performed by the University of Alberta Microanalysis Laboratory. Several compounds failed to afford consistent elemental analysis,<sup>12</sup> even when the combustion was performed on highly purified samples suitable for X-ray crystallography.

In the assignment of  $^1\text{H}$  NMR and  $^{13}\text{C}$  NMR spectra, the numbering scheme used for the 2-*N,N*-dimethylaminoindenyl

(10) Carter, C. A. G.; McDonald, R.; Stryker, J. M. *Organometallics* **1999**, *18*, 820.

(11) The full synthetic scope and applications of the bis(2-*N,N*-dimethylaminoindenyl)titanium(III) template will be detailed in a separate account.

(12) For a comment on this problem, common to certain classes of early transition metal complexes, see the supporting material in: Carney, M. J.; Walsh, P. J.; Bergman, R. G. *J. Am. Chem. Soc.* **1990**, *112*, 6426.

(6) Costa, E. M.; Stryker, J. M. Unpublished results.

(7) Carter, C. A. G. Ph.D. Dissertation, University of Alberta, 1998.

(8) Infrared spectroscopy has been used to suggest that the allylic ligands are  $\eta^3$ -coordinate in  $(\text{C}_5\text{Me}_5)_2\text{Ti}(\text{C}_3\text{H}_4\text{R})$  (R = H, Me): Luinstra, G. A.; ten Cate, L. C.; Heeres, H. J.; Pattiasina, J. W. Meetsma, A.; Teuben, J. H. *Organometallics* **1991**, *10*, 3227.

(9) Changes in allyl ligand coordination from  $\eta^3$ - to  $\eta^1$ - or to  $\eta^1, \eta^2$ - ( $\sigma, \pi$ )-bonding upon addition of alkyl substituents are common in d<sup>0</sup>-metallocene complexes of zirconium and titanium. Regardless of the thermodynamic coordination mode, the allylic ligands in such d<sup>0</sup>-complexes are kinetically labile, undergoing rapid  $\eta^3 \leftrightarrow \eta^1$  equilibration. See: (a) Martin, H. A.; Lemaire, P. J.; Jellinek, F. J. *Organomet. Chem.* **1968**, *14*, 149. (b) Yasuda, H.; Kajihara, Y.; Mashima, K.; Nagasuna, K.; Nakamura, A. *Chem. Lett.* **1981**, 671. Mashima, K.; Yasuda, H.; Asami, K.; Nakamura, A. *Chem. Lett.* **1983**, 219. (c) Blenkins, J.; de Liefde Meijer, H. J.; Teuben, J. H. J. *Organomet. Chem.* **1981**, *218*, 383. (d) McDade, C.; Bercaw, J. E. *J. Organomet. Chem.* **1985**, *279*, 281. (e) Highcock, W. J.; Mills, R. M.; Spencer, J. L.; Woodward, P. *J. Chem. Soc., Dalton Trans.* **1986**, 829, and references therein. (f) Larson, E. J.; van Dort, P. C.; Lakanen, J. R.; O'Neill, D. W.; Pederson, L. M.; McCandless, J. J.; Silver, M. E.; Russo, S. O.; Huffman, J. D. *Organometallics* **1988**, *7*, 1183. Vance, P. J.; Prins, T. J.; Hauger, B. E.; Silver, M. E.; Wemple, M. E.; Pederson, L. M.; Kort, D. A.; Kannisto, M. R.; Geerligs, S. J.; Kelly, R. S.; McCandless, J. J.; Huffman, J. D.; Peters, D. G. *Organometallics* **1991**, *10*, 917. (g) Tjaden, E. B.; Stryker, J. M. *J. Am. Chem. Soc.* **1993**, *115*, 2083.

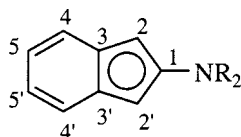


**Figure 1.** Numbering scheme for NMR spectroscopy of the *N,N*-dialkylaminoindenyl ligand system.

ligand is illustrated in Figure 1. Primes are used to designate symmetry-imposed inequivalency of aryl positions. In complexes where additional aromatic resonances overlap with the indenyl resonances, a ubiquitous designation of "aryl" is used.

**Bis(2-*N,N*-dimethylaminoindenyl)titanium Chloride (5).** In a Schlenk flask under an inert atmosphere, 2-*N,N*-dimethylaminoindene<sup>13</sup> (3.502 g, 22.0 mmol) was dissolved in 30 mL of THF and cooled to  $-40^{\circ}\text{C}$ . *n*-Butyllithium (23.1 mmol, 1.6 M) was added dropwise by syringe, and the solution was stirred at  $-40^{\circ}\text{C}$  for 3 h before warming to room temperature. In a separate Schlenk flask,  $\text{TiCl}_3 \cdot 3\text{THF}$ <sup>14</sup> (4.100 g, 11.0 mmol) was suspended in 40 mL of THF. The solution of 2-*N,N*-dimethylaminoindenyl lithium was transferred at room temperature via cannula into the titanium solution and left to stir overnight. After 12 h the solvent was removed under reduced pressure from the deep green solution, yielding a red-brown residue. The residue was extracted into benzene and the solution filtered through a sintered glass funnel layered with a short plug of Celite. The benzene was removed under reduced pressure, and the residual solid was crystallized from THF/hexane (1:2) at  $-35^{\circ}\text{C}$ , yielding the product as an amorphous terra-cotta red solid, sparsely sprinkled with green crystals (total 4.05 g, ~92% estimated<sup>15</sup>). Slow recrystallization from a dilute solution of THF layered with hexane and cooled to  $-35^{\circ}\text{C}$  gave a low recovery of green single crystals suitable for analysis by X-ray crystallography, establishing the structure as the lithium chloride adduct, bis(2-*N,N*-dimethylaminoindenyl)titanium chloride·(lithium chloride·2THF)·5·LiCl·(THF)<sub>2</sub>. To obtain LiCl-free product, the crude material (or the purified complex 5·LiCl(THF)<sub>2</sub>) was exhaustively desolvated under high vacuum ( $10^{-5}$  Torr), taken up into benzene, filtered to remove the insoluble lithium chloride, and "crystallized" from THF layered with hexane (1:4), giving complex 5 as an amorphous (and presumably dimeric) red solid (~90% yield). HRMS calcd for  $\text{C}_{22}\text{H}_{24}\text{N}_2\text{Ti}^{37}\text{Cl}$ :  $m/z$  401.10779, found 401.10803;  $\text{C}_{22}\text{H}_{24}\text{N}_2\text{Ti}^{35}\text{Cl}$   $m/z$  399.11075, found 399.11036. Anal. Calcd for  $\text{C}_{22}\text{H}_{24}\text{N}_2\text{TiCl}$ : C, 66.10; H, 6.05; N, 7.01. Found: C, 66.08; H, 6.11; N, 6.53.

**Bis(2-*N,N*-dimethylaminoindenyl)titanium Dichloride (6).** A sample of the crude monochloride complex (0.050 g, 0.125 mmol, assuming the mixture to consist only of the major product 5) was oxidized using  $\text{PbCl}_2$  (0.0174 g, 0.5 equiv) in THF at room temperature overnight. The residual lead was removed via filtration, and the remaining solution was concentrated and cooled to  $-35^{\circ}\text{C}$  to give the corresponding diamagnetic dichloride complex 6 as lustrous black crystals (0.053 g, near quantitative). <sup>1</sup>H NMR (200 MHz,  $\text{C}_6\text{D}_6$ ):  $\delta$  7.60 (m, second order, 4H, H4/5), 6.91 (m, second order, 4H, H4/5), 4.57 (br s, 4H, H2), 2.39 (s, 6H, N(CH<sub>3</sub>)<sub>2</sub>). <sup>13</sup>C NMR (50.3 MHz,  $\text{C}_6\text{D}_6$ ):  $\delta$  160.4 (C1), 128.3 (C3) 125.8 (C4/5), 123.7 (C4/5), 92.1 (C2), 39.2 (N(CH<sub>3</sub>)<sub>2</sub>). HRMS calcd for  $\text{C}_{22}\text{H}_{24}\text{N}_2\text{Ti}^{35}\text{Cl}_2$ :  $m/z$  434.07959, found 434.07940. Anal. Calcd: C, 60.46; H, 5.52; N, 6.63. Found: C, 60.05; H, 5.66; N, 6.42.

**Bis(2-*N,N*-dimethylaminoindenyl)titanium( $\eta^3$ -1-phenylallyl) (4a).** In the drybox, a vial containing a THF solution (10 mL) of bis(2-*N,N*-dimethylaminoindenyl)titanium chloride, 5 (255.5 mg, 0.639 mmol), was cooled to  $-35^{\circ}\text{C}$ . A

cooled THF (5 mL) solution ( $-35^{\circ}\text{C}$ ) of cinnamyl lithium<sup>16</sup> (87.0 mg, 0.703 mmol) was added, and the resulting solution was allowed to warm to room temperature and stir overnight. The THF was removed under reduced pressure, leaving a dark green residue. The product was extracted into benzene and filtered through a sintered glass funnel layered with a short plug of Celite. The benzene was removed in vacuo, and the resulting solid was crystallized from THF layered with hexane (1:3) cooled to  $-35^{\circ}\text{C}$ , affording dark green diamond-shaped crystals (225 mg, 73%). IR ( $\text{cm}^{-1}$ , cast (THF)): 2949 (m), 2866 (m), 2837 (m), 2796 (m), 1592 (s), 1544 (vs), 1528 (vs), 1486 (m), 1449 (m), 1429 (s), 1360 (s), 1251 (m), 1125 (m), 1066 (m), 988 (m), 803 (s), 787 (m), 739 (vs), 695 (m). HRMS calcd for  $\text{C}_{31}\text{H}_{33}\text{N}_2\text{Ti}$ :  $m/z$  481.21191, found 481.2123. Anal. Calcd: C, 77.43; H, 6.91; N, 5.82. Found: C, 77.21; H, 7.28; N, 5.69. Crystals suitable for X-ray diffraction were obtained from a dilute solution of the complex in THF layered with hexane and cooled to  $-35^{\circ}\text{C}$ .

**Bis(2-*N,N*-dimethylaminoindenyl)titanium( $\eta^3$ -1-methylallyl) (4b).** In the drybox, a vial containing a THF solution (5 mL) of bis(2-*N,N*-dimethylaminoindenyl)titanium chloride, 5 (57.5 mg, 0.144 mmol), was cooled to  $-35^{\circ}\text{C}$ . Crotylmagnesium chloride (0.100 mL, 1.5 M in THF, prepared from crotyl chloride and activated magnesium<sup>17</sup>) was diluted in THF (5 mL) and cooled to  $-35^{\circ}\text{C}$ . The two solutions were mixed together, allowed to warm to room temperature, and stirred for an additional 3 h. Removal of the THF in vacuo gave a dark red viscous oil, which was extracted into benzene and filtered through a sintered glass funnel layered with a short plug of Celite. The benzene was removed under reduced pressure. Purification of the residue from diethyl ether/hexane (1:5) gave a very dark red oil (39.8 mg, 66%). IR ( $\text{cm}^{-1}$ , cast (pentane)): 2931 (s), 2800 (m), 1588 (vs), 1548 (vs), 1529 (s), 1486 (m), 1449 (m), 1384 (m), 1362 (m), 1261 (w), 1126 (s), 1060 (s), 991 (w), 802 (m), 747 (m), 698 (m), 625 (m). Anal. Calcd: C, 74.45; H, 7.45; N, 6.68. Found: (trial 1) C, 71.87; H, 7.45; N, 6.15; (trial 2) C, 71.60; H, 7.39; N, 6.11. Crystals suitable for X-ray diffraction were obtained by repeated crystallization from dilute solutions of diethyl ether and hexane.

**3-Isopropyl-2-phenylbis(2-piperidinoindenyl)titanacyclobutane (7).** This procedure, modified from our previous report,<sup>10</sup> was used to obtain material suitable for crystallographic analysis. In the drybox, a vial containing bis(2-piperidinoindenyl)titanium( $\eta^3$ -1-phenylallyl) (48.9 mg, 0.0870 mmol), 3a, in THF (3 mL) was cooled to  $-35^{\circ}\text{C}$ . A solution of  $\text{SmI}_2$  (0.91 mL, 0.1 M in THF), cooled to  $-35^{\circ}\text{C}$ , was added, followed immediately by the addition of isopropyl iodide (9.1  $\mu\text{L}$  in 2 mL of THF, cooled to  $-35^{\circ}\text{C}$ ). The solution was allowed to warm to room temperature and stir for 5 h. The solvent was removed in vacuo and the crude product extracted into benzene/hexane (1:2) and filtered through a sintered glass funnel layered with Celite. The solvents were removed, and the resulting solid was crystallized at  $-35^{\circ}\text{C}$  by layering pentane on a solution of the complex in diethyl ether and

(16) Preparation of cinnamyl lithium: In a Schlenk flask, a THF solution (25 mL) of freshly distilled allyl benzene (5.0 mL, 37.7 mmol) was cooled to  $-78^{\circ}\text{C}$ . *n*-Butyllithium (18.1 mL, 2.5 M in hexanes) was transferred via cannula into the flask, and the reaction mixture was left to stir for 1 h at  $-78^{\circ}\text{C}$ . The reaction mixture was allowed to warm to room temperature and stirred for an additional hour. Removal of the solvent in vacuo yielded a yellow solid residue, which was washed repeatedly with hexane ( $4 \times 25$  mL) to give a brilliant yellow powder (3.98 g, 85%). This material was used without further characterization.

(17) Preparation of crotylmagnesium chloride with activated magnesium: In a Schlenk flask, 50 mL of dry THF was added to magnesium turnings (5.0 g) that had previously been vigorously stirred for 6 h under a nitrogen atmosphere (Baker, K. V.; Brown, J. M.; Hughes, N.; Skarnulis, A. J.; Sexton, A. *J. Org. Chem.* **1991**, *56*, 698). Crotyl chloride (5.0 mL in 15 mL of THF) was added dropwise to the turnings over the course of 4 h. The solution was left to stir for 14 h and then allowed to settle. The supernatant was removed via cannula and the concentration determined by titration of 100  $\mu\text{L}$  aliquots of the Grignard with 0.18 M menthol in  $\text{Et}_2\text{O}$  using 1,10-phenanthroline as an indicator.

(13) Edlund, U. *Acta Chem. Scand.* **1973**, *27*, 4027.

(14) Manzer, L. E. *Inorg. Synth.* **1982**, *21*, section 31.

(15) The molar ratio of complex 5 to complex 5·LiCl(THF)<sub>2</sub> could not be determined precisely; the yield of the reaction is estimated assuming conversion to complex 5 alone, the major material isolated in this procedure. The actual yield of the reaction is lower.

cooling to  $-35\text{ }^{\circ}\text{C}$ , yielding the known titanacyclobutane complex **7**<sup>10</sup> as diffractable deep red platelets (40.2 mg, 78%).

**3-Isopropyl-2-phenylbis(2-*N,N*-dimethylaminoindenyl)-titanacyclobutane (8).** In the drybox, a vial containing bis(2-*N,N*-dimethylaminoindenyl)titanium(*η*<sup>3</sup>-1-phenylallyl) (103.9 mg, 0.216 mmol), **4a**, in THF (5 mL) was cooled to  $-35\text{ }^{\circ}\text{C}$ . A cold ( $-35\text{ }^{\circ}\text{C}$ ) solution of  $\text{SmI}_2$  (2.25 mL, 0.1 M in THF) was added followed immediately by a cold solution of isopropyl iodide (22.6  $\mu\text{L}$  in 1 mL of THF). The reaction mixture was allowed to warm to room temperature and stir overnight. Almost immediately upon warming, the blue-green color of the solution began to dissipate, followed by the emergence of a dark chocolate brown solution. Only a very small quantity of Sm(III) precipitate was produced during the course of the reaction. The solvent was removed in vacuo and the brown residue extracted into benzene/hexane (1:2). The resultant solution was filtered through a sintered glass funnel layered with a short plug of Celite. The solvents were removed in vacuo, and the resulting residue was crystallized from THF/hexane (1:4) at  $-35\text{ }^{\circ}\text{C}$  to yield titanacyclobutane complex **8** as deep red rhomboid crystals (100.1 mg, 88%). <sup>1</sup>H NMR (400 MHz,  $\text{C}_6\text{D}_6$ , RT):  $\delta$  7.48 (m, 1H, H4/5), 7.32 (m, 4H, H4/5,  $\text{C}_6\text{H}_5$ ), 7.00 (t,  $J = 7.3$  Hz, 1H,  $\text{C}_6\text{H}_5$ ), 6.95 (ddd,  $J = 8.1$ , 6.9, 1.0 Hz, 1H,  $\text{C}_6\text{H}_5$ ), 6.90 (m, 4H, H4/5), 6.74 (ddd,  $J = 8.1$ , 6.7, 0.9 Hz, 1H,  $\text{C}_6\text{H}_5$ ), 6.12 (d,  $J = 8.0$  Hz, 1H,  $\text{C}_6\text{H}_5$ ), 5.41 (d,  $J = 1.7$  Hz, 1H, H2), 5.31 (d,  $J = 2.3$  Hz, 1H, H2'), 4.27 (br s, 1H, H2''), 4.05 (br s, 1H, H2'''), 3.32 (d,  $J = 10.7$  Hz, 1H,  $\alpha\text{-CH}(\text{C}_6\text{H}_5)$ ), 2.65 (t,  $J = 9.0$  Hz, 1H,  $\alpha\text{-CH}_2$ ), 2.36 (s, 6H,  $\text{N}(\text{CH}_3)_2$ ), 2.23 (s, 6H,  $\text{N}(\text{CH}_3)_2$ ), 1.50 (m, 1H,  $\text{CH}(\text{CH}_3)_2$ ), 1.15 (d,  $J = 6.6$  Hz, 3H,  $\text{CH}(\text{CH}_3)_2$ ), 1.05 (d,  $J = 6.7$  Hz,  $\text{CH}(\text{CH}_3)_2$ ), 1.04 (overlapping multiplet with  $\delta$  1.05, 1H,  $\beta\text{-CH}$ ), 0.61 (br s, 1H,  $\alpha\text{-CH}_2$ ). <sup>1</sup>H NMR (400 MHz,  $\text{C}_6\text{D}_6$ ,  $70\text{ }^{\circ}\text{C}$ ):  $\delta$  7.50 (m, 1H, aryl), 7.38 (d,  $J = 7.5$  Hz, 2H, aryl), 7.33 (t,  $J = 7.4$  Hz, 2H, aryl), 7.02 (t,  $J = 8.2$  Hz, 4H, aryl), 6.94 (m, 2H, aryl) 6.76 (t,  $J = 7.5$  Hz, 1H,  $\text{C}_6\text{H}_5$ ), 6.19 (d,  $J = 8.2$  Hz, 1H,  $\text{C}_6\text{H}_5$ ), 5.44 (d,  $J = 2.3$  Hz, 1H, H2), 5.42 (d,  $J = 2.3$  Hz, 1H, H2'), 4.44 (d,  $J = 2.0$  Hz, 1H, H2''), 4.19 (d,  $J = 2.2$  Hz, 1H, H2'''), 3.28 (d,  $J = 10.7$  Hz, 1H,  $\alpha\text{-CH}(\text{C}_6\text{H}_5)$ ), 2.61 (t,  $J = 9.0$  Hz, 1H,  $\alpha\text{-CH}_2$ ), 2.43 (s, 6H,  $\text{N}(\text{CH}_3)_2$ ), 2.38 (s, 6H,  $\text{N}(\text{CH}_3)_2$ ), 1.57 (septet, 1H,  $J = 7.0$  Hz,  $\text{CH}(\text{CH}_3)_2$ ), 1.16 (d,  $J = 6.5$  Hz, 3H,  $\text{CH}(\text{CH}_3)_2$ ), 1.10 (overlapping multiplet with  $\delta$  1.16 and 1.06, 1H,  $\beta\text{-CH}$ ), 1.06 (d,  $J = 6.5$  Hz, 3H,  $\text{CH}(\text{CH}_3)_2$ ), 0.56 (t,  $J = 9.6$  Hz, 1H,  $\alpha\text{-CH}_2$ ); (400 MHz,  $\text{C}_6\text{D}_6$ ,  $-60\text{ }^{\circ}\text{C}$ ) three rotational isomers of **8** are observed in a 2:2:1 ratio. Due to this complexity, complete assignment of this spectrum was not attempted. <sup>13</sup>C NMR (100.6 MHz,  $\text{C}_6\text{D}_6$ , RT, assignments by HMQC):  $\delta$  155.4 (C1), 152.0 ( $\text{C}_{\text{aryl}}$ ), 151.4 (C1'), 125.5 ( $\text{C}_{\text{aryl}}$ ), 125.1 ( $\text{C}_{\text{aryl}}$ ), 125.0 ( $\text{C}_{\text{aryl}}$ ), 124.7 ( $\text{C}_{\text{aryl}}$ ), 123.3 ( $\text{C}_{\text{aryl}}$ ), 123.0 ( $\text{C}_{\text{aryl}}$ ), 122.4 ( $\text{C}_{\text{aryl}}$ ), 121.7 ( $\text{C}_{\text{aryl}}$ ), 121.0 ( $\text{C}_{\text{aryl}}$ ), 120.7 ( $\text{C}_{\text{aryl}}$ ), 119.3 ( $\text{C}_{\text{aryl}}$ ), 91.4 (C2), 90.0 (C2'), 89.9 (C2''), 87.6 ( $\text{CH}(\text{C}_6\text{H}_5)$ ), 86.0 (C2'''), 80.0 ( $\alpha\text{-CH}_2$ ), 40.5 ( $\text{N}(\text{CH}_3)_2$ ), 39.5 ( $\text{N}(\text{CH}_3)_2$ ), 36.1 ( $\text{CH}(\text{CH}_3)_2$ ), 26.5 ( $\beta\text{-CH}$ ), 23.5 ( $\text{CH}(\text{CH}_3)_2$ ), 21.5 ( $\text{CH}(\text{CH}_3)_2$ ). <sup>1</sup>H NMR spectroscopy revealed that the isolated crystals retained a substoichiometric amount of coordinated THF. Anal. Calcd for a THF adduct,  $\text{C}_{34}\text{H}_{40}\text{N}_2\text{Ti}\cdot\text{C}_4\text{H}_8\text{O}$ : C, 76.49; H, 8.11; N, 4.69. Anal. Calcd for  $\text{C}_{34}\text{H}_{40}\text{N}_2\text{Ti}$ : C, 77.85; H, 7.69; N, 5.34. Found: C, 76.92; H, 7.98; N, 5.19.

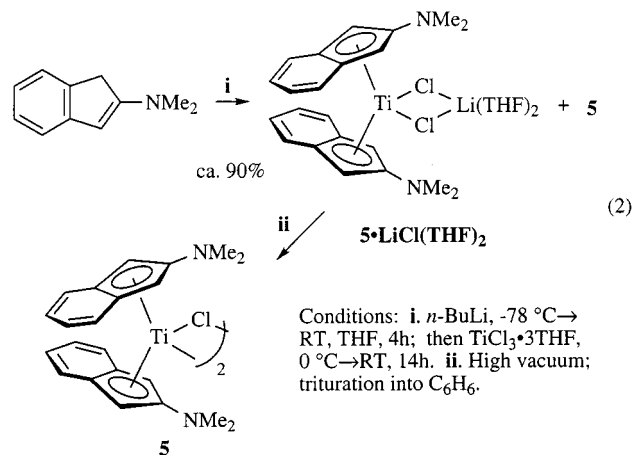
**3-Isopropyl-2-methylbis(2-*N,N*-dimethylaminoindenyl)-titanacyclobutane (9).** In the drybox, a vial containing a THF solution (5 mL) of bis(2-*N,N*-dimethylaminoindenyl)-titanium chloride (75.9 mg, 0.190 mmol), **5**, was cooled to  $-35\text{ }^{\circ}\text{C}$ . Crotylmagnesium chloride (128  $\mu\text{L}$ , 1.5 M in THF) was diluted in 5 mL of THF and cooled to  $-35\text{ }^{\circ}\text{C}$ . The two solutions were mixed together, allowed to warm to room temperature, and left to stir for an additional hour. The reaction mixture was recooled to  $-35\text{ }^{\circ}\text{C}$ , and a cooled solution of  $\text{SmI}_2$  (1.90 mL, 0.1 M in THF) was added, followed immediately by a cooled solution of isopropyl iodide (19.2  $\mu\text{L}$  in 2 mL of THF). The solution was warmed to room temperature and stirred for 30 min. Almost immediately, the blue color of the  $\text{SmI}_2$  began to dissipate, followed by the emergence of a purple-red solution

and a bright yellow precipitate of samarium(III). The solution was decanted from the precipitate and the solvent removed in vacuo. The residue was triturated with pentane and the solution filtered through a sintered glass funnel layered with a short plug of Celite. The pentane solution was concentrated to approximately half its original volume and cooled to  $-35\text{ }^{\circ}\text{C}$ , yielding dark purple microcrystals (56.3 mg, 68%). <sup>1</sup>H NMR (400 MHz,  $\text{C}_6\text{D}_6$ ):  $\delta$  7.48 (m, second order, 4H, H4/5), 7.06 (dt,  $J = 8.1$ , 0.8 Hz, 1H, H4/5), 6.97 (m, second order, 3H, H4/5), 5.34 (d,  $J = 2.2$  Hz, 1H, H2), 5.10 (d,  $J = 2.3$  Hz, 1H, H2'), 4.15 (d,  $J = 2.2$  Hz, 1H, H2''), 4.07 (d,  $J = 2.2$  Hz, 1H, H2'''), 2.46 (t,  $J = 9.1$  Hz, 1H,  $\alpha\text{-CH}_2$ ), 2.31 (s, 6H,  $\text{N}(\text{CH}_3)_2$ ), 2.29 (s, 6H,  $\text{N}(\text{CH}_3)_2$ ), 2.22 (dq,  $J = 6.9$ , 9.9 Hz, 1H,  $\alpha\text{-CH}(\text{CH}_3)$ ), 1.83 (d,  $J = 6.9$  Hz, 3H,  $\alpha\text{-CH}(\text{CH}_3)$ ), 1.71 (octet,  $J = 6.7$  Hz, 1H,  $\text{CH}(\text{CH}_3)_2$ ), 1.24 (d,  $J = 6.7$  Hz, 3H,  $\text{CH}(\text{CH}_3)_2$ ), 1.18 (d,  $J = 6.6$  Hz, 3H,  $\text{CH}(\text{CH}_3)_2$ ), 0.79 (t,  $J = 9.7$  Hz, 1H,  $\alpha\text{-CH}_2$ ),  $-0.015$  (dq,  $J = 9.9$ , 6.5 Hz, 1H,  $\beta\text{-CH}$ ). <sup>13</sup>C NMR (100 MHz,  $\text{C}_6\text{D}_6$ , assignments by HMQC):  $\delta$  163.9 (C1), 150.6 (C1'), 126.0, 125.4, 124.6, 123.9, 122.4, 122.1, 121.9, 121.7, 121.3, 120.5, 119.5, 119.4 (all C3/4/5), 91.7 (C2), 87.9 (C2'), 86.9 (C2''), 85.5 (C2'''), 83.4 ( $\alpha\text{-CH}(\text{CH}_3)$ ), 77.8 ( $\alpha\text{-CH}_2$ ), 40.1 ( $\text{N}(\text{CH}_3)_2$ ), 39.6 ( $\text{N}(\text{CH}_3)_2$ ), 34.6 ( $\text{CH}(\text{CH}_3)_2$ ), 31.5 ( $\beta\text{-CH}$ ), 27.4 ( $\text{CH}(\text{CH}_3)_2$ ), 23.8 ( $\text{CH}(\text{CH}_3)_2$ ), 21.2 ( $\text{CH}(\text{CH}_3)_2$ ). Anal. Calcd: C, 75.31; H, 8.28; N, 6.06. Found: C, 75.02; H, 8.33; N, 5.84.

**X-ray Crystal Structures of the Compounds 4a, 4b, 5•LiCl(THF)<sub>2</sub>, 7, and 8.** Crystal data and data collection and processing parameters are given in Table 1. The intensity data were collected on a Bruker P4/RA/SMART 1000 CCD<sup>18</sup> at  $-80\text{ }^{\circ}\text{C}$  with Mo K $\alpha$  radiation. In each case a semiempirical absorption correction was applied to the data. All crystal structures were solved using direct methods (SHELXS-86)<sup>19</sup> and refined against  $F^2$  using SHELXL-93.<sup>20</sup> All non-hydrogen atoms were refined anisotropically. Complete data are provided as Supporting Information.

## Results

**Syntheses of Bis(2-*N,N*-dimethylaminoindenyl)-Ti(III) Complexes.** The synthesis of bis(2-*N,N*-dimethylaminoindenyl)titanium chloride, **5**, was accomplished by in situ lithiation of 2-*N,N*-dimethylaminoindenene with *n*-butyllithium in THF and slow addition of this solution to a suspension of  $\text{TiCl}_3\cdot 3\text{THF}$  at room temperature (eq 2). The addition of isolated 2-*N,N*-



dimethylaminoindenyllithium as an amorphous solid to

(18) Programs for diffractometer operation, data collection, data reduction and absorption correction were those supplied by Bruker.  
 (19) Sheldrick, G. M. *Acta Crystallogr.* **1990**, *A46*, 467.  
 (20) Sheldrick, G. M. *SHELXL-93*. Program for crystal structure determination; University of Göttingen, Germany, 1993.

**Table 1. Crystallographic Experimental Details**

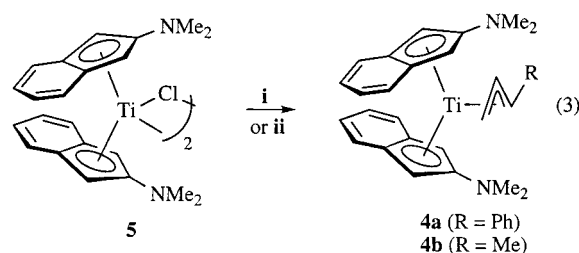
	<b>4a</b>	<b>4b</b>	<b>5·LiCl(THF)<sub>2</sub></b>	<b>7</b>	<b>8</b>
formula	C <sub>31</sub> H <sub>33</sub> N <sub>2</sub> Ti	C <sub>26</sub> H <sub>31</sub> N <sub>2</sub> Ti	C <sub>30</sub> H <sub>40</sub> Cl <sub>2</sub> LiN <sub>2</sub> O <sub>2</sub> Ti	C <sub>40</sub> H <sub>48</sub> N <sub>2</sub> Ti	C <sub>34</sub> H <sub>40</sub> N <sub>2</sub> Ti
fw	481.49	419.43	586.38	604.70	524.58
cryst dimens (mm)	0.27 × 0.21 × 0.08	0.45 × 0.27 × 0.09	0.37 × 0.14 × 0.14	0.16 × 0.16 × 0.06	0.28 × 0.26 × 0.14
cryst syst	orthorhombic	monoclinic	monoclinic	triclinic	triclinic
space group	<i>Pbca</i> (No. 61)	<i>C2/c</i> (No. 15)	<i>C2/c</i> (No. 15)	<i>P</i> $\bar{1}$ (No. 2)	<i>P</i> $\bar{1}$ (No. 2)
unit cell params					
<i>a</i> (Å)	9.8686(15)	28.790(4)	16.0060(15)	11.6351(8)	9.2259(6)
<i>b</i> (Å)	18.510(3)	8.1016(12)	11.6875(12)	12.5204(8)	11.4486(8)
<i>c</i> (Å)	27.427(4)	20.223(3)	17.1235(15)	11.7615(8)	13.1688(9)
$\alpha$ (deg)				83.0481(13)	91.9270(10)
$\beta$ (deg)		111.707(3)	109.2334(19)	88.1276(12)	92.8130(10)
$\gamma$ (deg)				72.7920(13)	93.0000(10)
<i>V</i> (Å <sup>3</sup> )	5010.1(13)	4382.4(11)	3024.5(5)	1624.63(19)	1386.44(16)
<i>Z</i>	8	8	4	2	2
$\rho_{\text{calcd}}$ (g cm <sup>-3</sup> )	1.277	1.271	1.288	1.236	1.257
$\mu$ (mm <sup>-1</sup> )	0.363	0.405	0.488	0.294	0.334
2 $\theta$ limit (deg)	51.50	51.40	52.74	51.50	51.40
total no. of data collected	25624 <sup>a</sup>	10604 <sup>b</sup>	7268 <sup>c</sup>	9065 <sup>d</sup>	7467 <sup>e</sup>
no. of ind reflns	4778	4162	3094	6155	5230
no. of observations ( <i>NO</i> )	1687	2321	2495	3813	3924
goodness-of-fit ( <i>S</i> ) <sup>f</sup>	0.838	0.882	1.039	0.887	1.035
final <i>R</i> indices <sup>g</sup>					
<i>R</i> <sub>1</sub> [ <i>F</i> <sub>o</sub> <sup>2</sup> ≥ 2 $\sigma$ ( <i>F</i> <sub>o</sub> <sup>2</sup> )]	0.0771	0.0451	0.0411	0.0482	0.0545
<i>wR</i> <sub>2</sub> [ <i>F</i> <sub>o</sub> <sup>2</sup> ≥ 3 $\sigma$ ( <i>F</i> <sub>o</sub> <sup>2</sup> )]	0.2237	0.0999	0.1104	0.1070	0.1540
largest diff peak and hole (e Å <sup>-3</sup> )	0.634 and -0.745	0.316 and -0.191	0.391 and -0.317	0.234 and -0.284	0.412 and -0.503

<sup>a</sup> (-11 ≤ *h* ≤ 12, -22 ≤ *k* ≤ 21, -33 ≤ *l* ≤ 30). <sup>b</sup> (-11 ≤ *h* ≤ 10, -13 ≤ *k* ≤ 13, -14 ≤ *l* ≤ 16). <sup>c</sup> (-20 ≤ *h* ≤ 17, -14 ≤ *k* ≤ 14, -8 ≤ *l* ≤ 21). <sup>d</sup> (-14 ≤ *h* ≤ 14, -15 ≤ *k* ≤ 14, -14 ≤ *l* ≤ 14). <sup>e</sup> (-23 ≤ *h* ≤ 34, -9 ≤ *k* ≤ 9, -24 ≤ *l* ≤ 24). <sup>f</sup> *S* = [Σ*w*(*F*<sub>o</sub><sup>2</sup> - *F*<sub>c</sub><sup>2</sup>)/(*n* - *p*)]<sup>1/2</sup> (*n* = number of data; *p* = number of parameters varied; *w* = [σ<sup>2</sup>(*F*<sub>o</sub><sup>2</sup>) + (0.0972*P*)<sup>-1</sup> where *P* = [max(*F*<sub>o</sub><sup>2</sup>, 0) + 2*F*<sub>c</sub><sup>2</sup>/3]. <sup>g</sup> *R*<sub>1</sub> = Σ|*F*<sub>o</sub> - |*F*<sub>c</sub>||/Σ|*F*<sub>o</sub>|; *wR*<sub>2</sub> = [Σ*w*(*F*<sub>o</sub><sup>2</sup> - *F*<sub>c</sub><sup>2</sup>)<sup>2</sup>/Σ*w*(*F*<sub>o</sub><sup>4</sup>)]<sup>1/2</sup>.

a suspension of TiCl<sub>3</sub>·3THF failed to give complex **5**, as did the use of 2-*N,N*-(dimethylamino)-1-trimethylsilylindene<sup>21a</sup> or 1-tributylstannyl-2-*N,N*-dimethylaminoindene<sup>21b</sup> as milder ligand transfer reagents. Initial crystallization of the product from THF layered with hexane gave a mixture of green crystals and an amorphous terra-cotta red solid in high yield.<sup>15</sup> Slow recrystallization of this mixture from THF afforded green single crystals suitable for X-ray crystallography. The complex was revealed to incorporate an equivalent of lithium chloride, as well as two THF ligands, completing the lithium coordination sphere (Figure 2). Upon thorough evacuation at high vacuum, the green crystals of complex **5**·LiCl(THF)<sub>2</sub> transformed into a terra-cotta red amorphous powder. This red powder was taken up into benzene, filtered to remove lithium chloride, and recrystallized to analytical purity. While the elemental analysis is consistent with assignment as bis(2-*N,N*-dimethylaminoindenyl)titanium chloride (**5**), we have not determined whether the salt-free complex is monomeric or dimeric.<sup>22</sup>

The cinnamyl ( $\eta^3$ -1-phenylallyl) and crotyl ( $\eta^3$ -1-methylallyl) complexes **4a** and **4b** were obtained upon treatment of complex **5** with cinnamyl lithium and crotylmagnesium chloride, respectively, at -35 °C in

THF (eq 3). The cinnamyl complex **4a** was isolated as a



Conditions: **i**. PhCH=CHCH<sub>2</sub>Li, -35 °C → RT, THF, 12h, 73%;  
**ii**. as for **i**. except CH<sub>3</sub>CH=CHCH<sub>2</sub>MgCl, 66%.

deep green crystalline material in 73% yield. This complex is mildly unstable and over the course of several months at room temperature decomposes to an intractable brown solid. The green color of complex **4a** is attributed to the extended conjugation afforded by the phenyl substituent on the allyl ligand; by comparison, the unsubstituted allyl complex is yellow.<sup>11</sup> Consistent with this hypothesis, bis(2-piperidinoindenyl)titanium-( $\eta^3$ -1-phenylallyl), **3a**, is also green.<sup>10</sup>

For the synthesis of crotyl complex **4b**, the use of crotylmagnesium bromide in place of the chloride results in a significantly lower yield. Obtaining single crystals of this complex proved to be very difficult, but repeated

(21) (a) The synthesis of 2-(*N,N*-dimethylamino)-1-(trimethylsilyl)indene was based on a method reported by Clark: Cardoso, A. M.; Clark, R. J.; Moorhouse, S. J. *J. Chem. Soc., Dalton Trans.* **1980**, 1156. Coordination of silylated cyclopentadienyl ligands to titanium: Winter, C. H.; Zhou, X.-X.; Dobbs, D. A.; Heeg, M. J. *Organometallics* **1991**, *10*, 210. (b) The synthesis of 1-tributylstannyl-2-*N,N*-dimethylaminoindene is based on the method described by Schlosser: Desponds, O.; Schlosser, M. J. *Organomet. Chem.* **1991**, *409*, 93. Coordination of cyclopentadienyl tin derivatives to titanium: Abel, E. W.; Moorhouse, S. J. *J. Chem. Soc., Dalton Trans.* **1973**, 1706. Jutzi, P.; Kuhn, M. J. *Organomet. Chem.* **1979**, *173*, 221. O'Hare, D.; Murphy, V.; Diamond, G. M.; Arnold, P.; Mountford, P. *Organometallics* **1994**, *13*, 4689. Hart, S. L.; Duncalf, D. J.; Hastings, J. J.; McCamley, A.; Taylor, P. C. *J. Chem. Soc., Dalton Trans.* **1996**, 2843.

(22) Titanocene(III) chloride complexes typically adopt monomeric structures in the case of sterically significant ancillary ligands and chloride-bridged dimers for complexes of smaller ligands. Monomeric complexes: Pattiasina, J. W.; Heeres, H. J.; van Bolhuis, F.; Meetsma, A.; Teuben, J. H. *Organometallics* **1987**, *6*, 1004. Castellani, M. P.; Geib, S. J.; Rheingold, A. L.; Trogler, W. C. *Organometallics* **1987**, *6*, 2524. Urazowski, I. F.; Ponomaryov, V. I.; Ellert, O. G.; Nifant'ev, I. E.; Lemenovskii, D. A. *J. Organomet. Chem.* **1988**, *356*, 181. Troyanov, S. I.; Rybakov, V. B.; Thewalt, U.; Varga, V.; Mach, K. J. *Organomet. Chem.* **1993**, *447*, 221. Dimeric complexes: Jungst, R.; Sekutowski, D.; Davis, J.; Luly, M.; Stucky, G. *Inorg. Chem.* **1977**, *16*, 1645. Martin, J.; Fauconet, M.; Moise, C. *J. Organomet. Chem.* **1989**, *371*, 87.

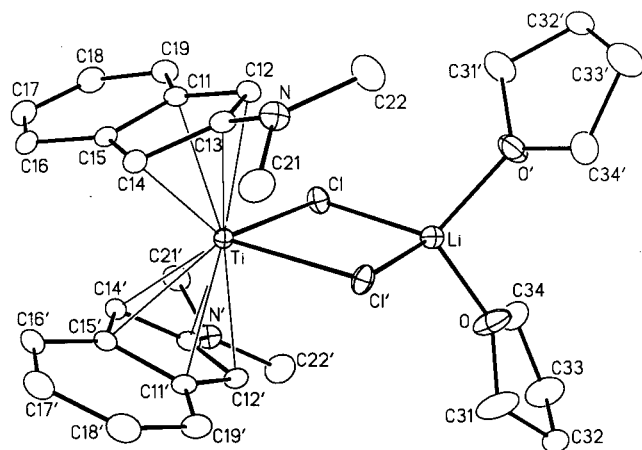


**Figure 2.** Molecular structure of complex **5**·LiCl(THF)<sub>2</sub>. Selected bond distances (Å) and angles (deg): Ti–Cl = 2.5184(6), Li–Cl = 2.284(4), Li–O = 1.923(4), Ti–C(11) = 2.4114(19), Ti–C(12) = 2.3855(19), Ti–C(13) = 2.517(2), Ti–C(14) = 2.400(2), Ti–C(15) = 2.443(2), N–C(13) = 1.372(3), N–C(21) = 1.456(3), N–C(22) = 1.448(3); Cl–Ti–Cl' = 84.97(3), Cl–Li–Cl' = 96.3(2), C(13)–N–C(21) = 119.18(19), C(13)–N–C(22) = 119.2(2), C(22)–N–C(21) = 117.0(2). Primed and unprimed atoms are related via the 2-fold rotational axis.

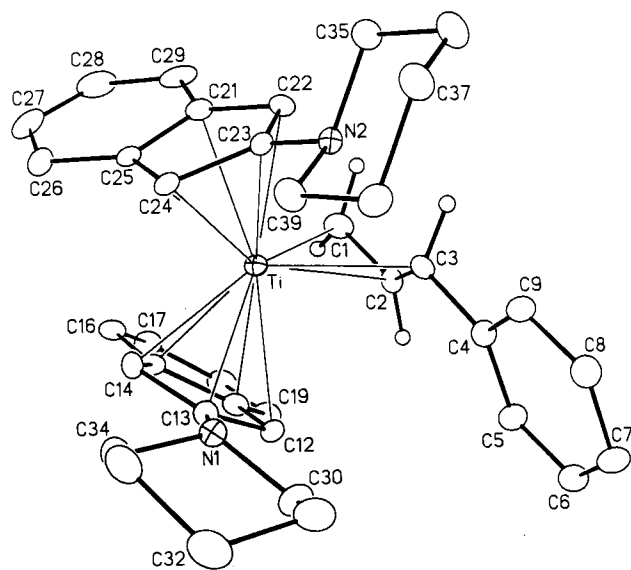


**Figure 3.** Molecular structure of **3a**.<sup>10</sup>

recrystallization from dilute solutions of diethyl ether carefully layered with hexane ultimately provided suitable single crystals. Combustion analysis of this very air sensitive compound was not within tolerance, a problem also observed for certain other oxophilic early metal complexes.<sup>12</sup>

**Crystallographic Analysis of Ti(III) Complexes 4a and 4b.** The solid-state molecular structure of cinnamyl complex **4a** together with the atomic labeling scheme is shown in Figure 4. The crotyl complex **4b** crystallizes as two equally abundant conformational isomers **4b** and **4b'**; the molecular structure of each conformer and the atomic labeling schemes are shown in Figure 5a,b. In the disordered crystal of the crotyl complex **4b/4b'**, two independent titanium atoms are defined, but only three independent indenyl ligands: the two conformational isomers share the orientation of one

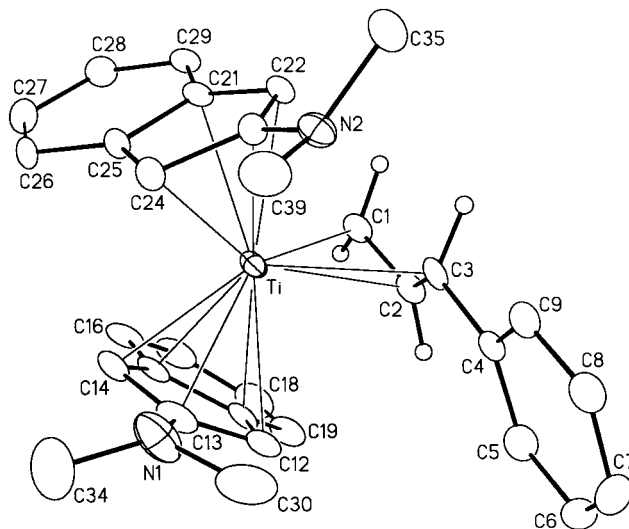


**Figure 4.** Molecular structure of **4a**. Selected interatomic distances are listed in Table 2.

indenyl ligand in the lattice, while the remaining ligand orientation differs markedly in the two isomers. Selected bond lengths and angles are presented in Table 2 for complex **4a** and in Table 3 for complexes **4b** and **4b'**.

The cinnamyl and crotyl substituents in the crystal structures of complexes **4a** and **4b** adopt the anticipated  $\eta^3$ -coordination, *syn* substituent stereochemistry, partially pyramidalized allyl terminal carbons and unsymmetrical coordination of the allyl carbon atoms to the metal.<sup>10,23</sup> The tilt angle that the allyl ligand plane makes with the Ti(III) template in complexes **4a**, **4b**, and **4b'** falls within the range reported for other Ti(III) allyl complexes (Table 4).<sup>23</sup> In complex **4a**, the shortened C3–C4 bond and the coplanarity of the phenyl and allyl  $\pi$ -systems suggest the presence of substantial conjugative stabilization within the cinnamyl ligand.

The relative spatial orientation of the 2-*N,N*-dimethylaminoindenyl ligands can be represented by the indenyl rotational angle parameter.<sup>24</sup> A measured indenyl rotation angle of 0° defines perfectly eclipsed (*syn*) indenyl rings; a 180° rotational angle is indicative of staggered (*anti*) indenyl rings. In cinnamyl complex **4a**, the two *N,N*-dimethylamino substituents are roughly *syn* to each other with a measured indenyl rotational angle of 41.9°. Despite the steric differences, the orientation of the ancillary ligands in 2-*N,N*-dimethylaminoindenyl complex **4a** is nearly identical to that determined for the 2-piperidinoindenyl cinnamyl complex **3a** (Figure 3), for which an indenyl rotation angle of 36.9° was determined.<sup>10</sup>

For the crotyl complex, the most significant difference between the two conformers **4b** and **4b'** is in the relative orientations of the ancillary ligands.<sup>25</sup> In conformer **4b**,

(23) (a) Helmholdt, R. B.; Jelinek, F.; Martin, H. A.; Vos, A. *Recl. Trav. Chim. Pays-Bas* **1967**, *86*, 1263. (b) Chen, J.; Kai, Y.; Nasai, N.; Yasuda, H.; Yamamoto, H.; Nakamura, A. *J. Organomet. Chem.* **1991**, *407*, 191.

(24) (a) Westcott, S. A.; Kakkar, A. K.; Stringer, G.; Taylor, N. J.; Marder, T. B. *J. Organomet. Chem.* **1990**, *394*, 777. (b) O'Hare, D.; Green, J. C.; Marder, T.; Collins, S.; Stringer, G.; Kakkar, A. T.; Kaltsoyannis, N.; Kuhn, A.; Lewis, R.; Mehnert, C.; Scott, P.; Kurmoo, M.; Pugh, S. *Organometallics* **1992**, *11*, 48. (c) O'Hare, D.; Murphy, V. J.; Kaltsoyannis, N. *J. Chem. Soc., Dalton Trans.* **1993**, 383. (d) O'Hare, D.; Murphy, V.; Diamond, G. M.; Arnold, P.; Mountford, P. *Organometallics* **1994**, *13*, 4689.

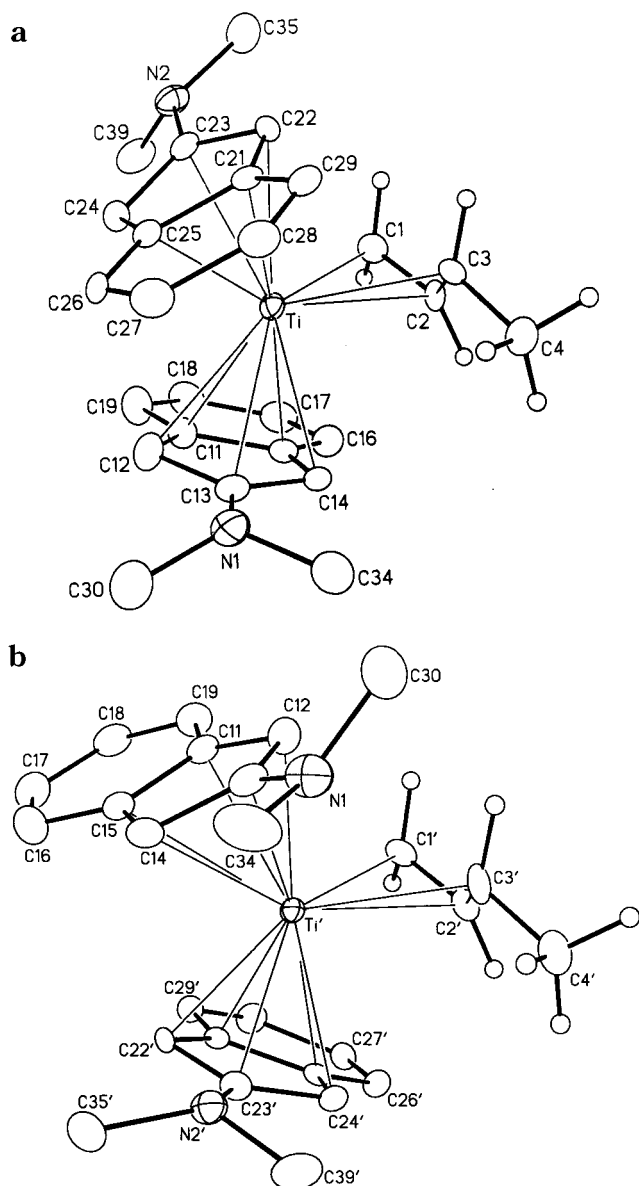


**Figure 5.** (a) Molecular structure of **4b**. Selected interatomic distances and angles are listed in Table 3. (b) Molecular structure of **4b'**. Selected interatomic distances and angles are listed in Table 3.

the indenyl ligands are oriented *anti*, with an indenyl rotational angle of 177.8°. In conformer **4b'**, the ancillary ligands approach a *syn* orientation with a corresponding indenyl rotational angle of 41.6°, almost identical to that observed in the cinnamyl complex **4a**.

Many indenyl complexes are prone to ring slippage away from the symmetrical  $\eta^5$ -coordination mode to  $\eta^3$ -coordination.<sup>24,26,27</sup> This allows the indenyl  $\pi$ -system to rehybridize, increasing the residual aromatic character of the indenyl arene ring. Three parameters have been devised to quantify these distortions:<sup>28</sup> (1) the slip parameter ( $\Delta_{M-C}$ ), (2) the hinge angle (HA), and (3) the fold angle (FA).<sup>26</sup> The slip parameter is a measure of the hapticity of indenyl coordination to the metal ( $\eta^5$ - to  $\eta^3$ -coordination) and is defined as the difference in

(25) Conformational disorder in the crystals of bis( $\eta^5$ -indenyl)-titanium(CO)<sub>2</sub> has also been reported: Rausch, M. D.; Moriarty, K. J.; Atwood, J. L.; Hunter, W. E. *J. Organomet. Chem.* **1987**, *327*, 39.

**Table 2.** Selected Bond Lengths (Å) and Angles (deg) for **4a**

Ti–C1	2.336(6)	N1–C13	1.399(9)
Ti–C2	2.364(6)	N1–C30	1.423(10)
Ti–C3	2.475(6)	N1–C34	1.371(9)
Ti–C11	2.488(6)	N2–C23	1.382(8)
Ti–C12	2.447(7)	N2–C35	1.464(7)
Ti–C13	2.434(7)	N2–C39	1.454(8)
Ti–C14	2.344(6)	C1–C2	1.420(9)
Ti–C15	2.428(6)	C2–C3	1.416(8)
Ti–C21	2.486(6)	C3–C4	1.451(9)
Ti–C22	2.437(6)	Ti–Cp(cent) <sup>a</sup>	2.108, 2.131
Ti–C24	2.370(6)	Ti–Cp(plane) <sup>b</sup>	2.105(3), 2.130(3)
Ti–C25	2.466(6)		
C1–Ti–C3	63.4(2)	C13–N1–C30	117.1(8)
C1–C2–C3	126.3(6)	C13–N1–C34	117.3(7)
C2–C3–C4	125.1(6)	C30–N1–C34	116.9(7)
Cp(cent)–M–Cp(cent) <sup>a</sup>	133.9	C23–N2–C35	115.9(6)
Cp(plane)–M–Cp(plane) <sup>b</sup>	50.6(3)	C23–N2–C39	116.7(6)
		C35–N2–C39	113.6(5)

<sup>a</sup> Centroid of the indenyl ligand. <sup>b</sup> Calculated normal to plane of indenyl ligand.

the average bond lengths of the metal to the ring-junction carbons, e.g., C(11) and C(15), and the metal to the adjacent carbon atoms of the five-membered ring, e.g., C(12), C(13), and C(14). The hinge angle measures distortions in the planarity of the cyclopentadienyl ring and is defined as the angle between the planes [C(12), C(13), C(14)] and [C(12), C(11), C(15), C(14)]. The fold angle is the angle between the two rings in the indenyl

(26)  $\eta^3$ -Indenyl coordination: (a) O'Connor, J. M.; Casey, C. P. *Chem. Rev.* **1987**, *87*, 307, and references therein. (b) Merola, J. S.; Kacmarcik, R. T.; Van Engen, D. J. *Am. Chem. Soc.* **1986**, *108*, 329. (c) Kowalewski, R. M.; Rheingold, A. L.; Trogler, W. C.; Basolo, F. *J. Am. Chem. Soc.* **1986**, *108*, 2460. (d) Forschner, T. C.; Cutler, A. R.; Kullnig, R. K. *Organometallics* **1987**, *6*, 889. (e) Poli, R.; Mattamana, S. P.; Falvello, L. R. *Gazz. Chim. Ital.* **1992**, *112*, 315. (f) Ascenso, J. R.; de Azevedo, C. G.; Gonçalves, I. S.; Herdtweck, E.; Moreno, D. S.; Romão, C. C.; Zühlke, J. *Organometallics* **1994**, *13*, 429. (g) Le Husebo, T.; Jensen, C. M. *Organometallics* **1995**, *14*, 1087. (h) Ascenso, J. R.; de Azevedo, C. G.; Gonçalves, I. S.; Herdtweck, E.; Moreno, D. S.; Pessanha, M.; Romão, C. C. *Organometallics* **1995**, *14*, 3901. (i) Kakkar, A. K.; Stringer, G.; Taylor, N. J.; Marder, T. B. *Can. J. Chem.* **1995**, *73*, 981. (j) Calhorda, M. J.; Gamelas, I. S.; Gonçalves, I. S.; Herdtweck, E.; Romão, C. C.; Veiros, L. F. *Organometallics* **1998**, *17*, 2597.

(27) Intermediate  $\eta^3$ - to  $\eta^5$ -indenyl coordination: see refs 24a, 26a, 26i and the following: (a) Marder, T. B.; Calabrese, J. C.; Roe, D. C.; Tulip, T. H. *Organometallics* **1987**, *6*, 2012. (b) Carl, R. T.; Hughes, R. P.; Rheingold, A. L.; Marder, T. B.; Taylor, N. J. *Organometallics* **1988**, *7*, 1613. (c) Kakkar, A. K.; Taylor, N. J.; Calabrese, J. C.; Nugent, W. A.; Roe, D. C.; Connaway, E. A.; Marder, T. B. *J. Chem. Soc., Chem. Commun.* **1989**, 990. (d) Kakkar, A. K.; Jones, S. F.; Taylor, N. J.; Collins, S.; Marder, T. B. *J. Chem. Soc., Chem. Commun.* **1989**, 1454. (e) Kakkar, A. K.; Taylor, N. J.; Marder, T. B.; Shen, J. K.; Hallinan, N.; Basolo, F. *Inorg. Chim. Acta* **1992**, *198–200*, 219. (f) Morandini, F.; Piloni, G.; Consiglio, G.; Sironi, A.; Moret, M.; *Organometallics* **1993**, *12*, 3495. (g) Frankcom, T. M.; Green, J. C.; Nagy, A.; Marder, T. B. *Organometallics* **1993**, *12*, 3688. (h) Rau, D.; Behrens, U.; *J. Organomet. Chem.* **1993**, *461*, 151. (i) Zhou, Z.; Jablonski, C.; Bridson, J. J. *Organomet. Chem.* **1993**, *461*, 215. (j) Westcott, A. S.; Stringer, G.; Anderson, S.; Taylor, N. J.; Marder, T. B. *Inorg. Chem.* **1994**, *33*, 4589. (k) Kakkar, A. K.; Stringer, G.; Taylor, N. J.; Marder, T. B. *Can. J. Chem.* **1995**, *73*, 981. (l) Comstock, M. C.; Shapley, R. J. *Organometallics* **1997**, *16*, 4816. (m) Bassetti, M.; Casellato, P.; Gamasa, M. P.; Gimeno, J.; González-Bernardo, C.; Martín-Vaca, B. *Organometallics* **1997**, *16*, 5470. (n) Stradiotto, M.; Hughes, D. W.; Bain, A. D.; Brook, M. A.; McGlinchey, M. J. *Organometallics* **1997**, *16*, 5563. (o) Huber, T. A.; Bayrakdarian, M.; Dion, S.; Dubuc, I.; Bélanger-Gariépy, F.; Zargarian, D. *Organometallics* **1997**, *16*, 5811. (p) Cecchetto, P.; Cecon, A.; Gambaro, A.; Santi, S.; Ganis, P.; Gobetto, R.; Valle, G.; Venzo, A. *Organometallics* **1998**, *17*, 752, and references therein. (q) Westcott, S. A.; Taylor, N. J.; Marder, T. B. *Can. J. Chem.* **1999**, *77*, 199. (r) Gamelas, C. A.; Herdtweck, E.; Lopes, J. P.; Romão, C. C. *Organometallics* **1999**, *18*, 506. (s) Calhorda, M. J.; Gamelas, C. A.; Romão, C. C.; Veiros, L. F. *Eur. J. Inorg. Chem.* **2000**, *2*, 331.

(28) Other workers have selected different, but related, parameters to quantify indenyl ligand distortions: Faller, J. W.; Crabtree, R. H.; Habib, A. *Organometallics* **1985**, *5*, 929.

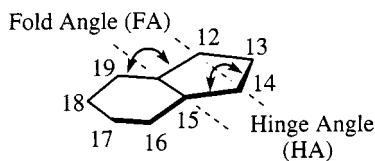
**Table 3. Selected Bond Lengths (Å) and Angles (deg) for 4b and 4b'**

Ti–C1	2.292(5)	Ti'–C1'	2.272(11)
Ti–C2	2.350(6)	Ti'–C2'	2.335(10)
Ti–C3	2.484(10)	Ti'–C3'	2.447(12)
Ti–C11	2.473(4)	Ti'–C11	2.432(4)
Ti–C12	2.537(4)	Ti'–C12	2.243(4)
Ti–C13	2.588(4)	Ti'–C13	2.362(4)
Ti–C14	2.401(4)	Ti'–C14	2.461(4)
Ti–C15	2.394(4)	Ti'–C15	2.566(4)
Ti–C21	2.453(5)	Ti'–C21'	2.411(4)
Ti–C22	2.425(8)	Ti'–C22'	2.323(4)
Ti–C23	2.506(6)	Ti'–C23'	2.454(9)
Ti–C24	2.403(13)	Ti'–C24'	2.457(5)
Ti–C25	2.432(11)	Ti'–C25'	2.496(7)
N1–C13	1.396(3)	N2'–C23'	1.408(13)
N1–C30	1.431(3)	N2'–C35'	1.453(8)
N1–C34	1.440(3)	N2'–C39'	1.430(11)
N2–C23	1.407(6)	C1'–C2'	1.402(15)
N2–C35	1.440(14)	C2'–C3'	1.45(3)
N2–C39	1.435(7)	C3'–C4'	1.46(3)
C1–C2	1.394(8)	Ti–Cp(cent) <sup>a</sup>	2.167, 2.124
C2–C3	1.354(11)	Ti'–Cp(cent) <sup>a</sup>	2.094, 2.107
C3–C4	1.519(15)	Ti–Cp(plane) <sup>b</sup>	2.1569(12), 2.133(5)
		Ti'–Cp(plane) <sup>b</sup>	2.073(3), 2.102(4)
C1–Ti–C3	61.3(3)	C1'–Ti'–C3'	64.8(6)
C1–C2–C3	125.1(6)	C1'–C2'–C3'	125.0(11)
C2–C3–C4	123.9(7)	C2'–C3'–C4'	120.1(16)
C13–N1–C30	118.5(2)		
C13–N1–C34	116.4(2)		
C30–N1–C34	115.1(2)		
C23–N2–C35	117.3(7)	C23'–N2'–C35'	118.2(7)
C23–N2–C39	117.2(5)	C23'–N2'–C39'	116.4(7)
C35–N2–C39	114.7(7)	C35'–N2'–C39'	116.2(8)
Cp(cent)–M–Cp(cent) <sup>a</sup>	133.2 (Ti), 131.2 (Ti')		
Cp(plane)–M–Cp(plane) <sup>b</sup>	42.9(3) (Ti), 45.27(15) (Ti')		

<sup>a</sup> Centroid of the indenyl ligand. <sup>b</sup> Calculated normal to plane of indenyl ligand.

**Table 4. Comparison of Allyl Bond Lengths (Å) and Angles (deg) for Ti(III) Complexes**

complex	tilt angle	Ti–C(1)	Ti–C(2)	Ti–C(3)	C(1)–C(2)	C(2)–C(3)	C(3)–C(4)
3a	111.8(6)	2.318(6)	2.351(6)	2.448(6)	1.387(8)	1.381(8)	1.480(8)
4a	113.2(5)	2.336(6)	2.364(6)	2.475(6)	1.420(9)	1.416(8)	1.451(9)
4b	110.0(6)	2.292(5)	2.350(6)	2.484(10)	1.394(8)	1.354(11)	1.519(15)
4b'	113.8(9)	2.272(11)	2.335(10)	2.447(12)	1.402(15)	1.45(3)	1.46(3)

**Figure 6.** Diagram illustrating the indenyl “hinge” and “fold” axes.

system and is defined by the difference in the planes of the five-membered ring, [C(12), C(11), C(15), C(14)], and the six-membered ring, [C(19), C(11), C(15), C(16)] (Figure 6). Values for these parameters range from less than 0.03 Å ( $\Delta_{M-C}$ ), 2.5° (HA), and 4.4° (FA) for “true”  $\eta^5$ -complexes<sup>24a</sup> to values greater than 0.8 Å ( $\Delta_{M-C}$ ) and 28° (FA) for “true”  $\eta^3$ -complexes,<sup>29</sup> with intermediate values of 0.11–0.43 Å ( $\Delta_{M-C}$ ), 7–14° (HA), and 6–13° (FA) observed for “distorted” complexes,<sup>27</sup> in which some degree of bonding occurs from the metal to the ring junction carbon atoms. These data have been calculated for complexes **3a**, **4a**, **4b**, and **4b'** and can be found in Table 5. In addition to these parameters, a symmetrically coordinated  $\eta^5$ -indenyl ring will have significant bond alternation in the internal (ring) carbon–

**Table 5. Structural Data for Indenyl Coordination**

complex	$\Delta_{M-C}$ (Å) <sup>a</sup>	fold angle (deg) <sup>b</sup>	hinge angle (deg) <sup>c</sup>
<b>3a</b>	0.0450	2.8(5)	6.3(8)
	0.0490	6.7(4)	8.5(8)
<b>4a</b>	0.0497	3.6(3)	5.9(4)
	0.0625	5.1(3)	8.9(6)
<b>4b</b>	0.0751	3.4(2)	7.3(2)
	0.0022	4.0(4)	9.4(6)
<b>4b'</b>	0.1437	3.4(2)	7.3(2)
	0.0422	3.0(2)	7.2(4)
<b>7</b>	0.0653	4.0 (2)	5.8(4)
	0.0313	5.4(2)	11.3(3)
<b>8</b>	0.0178	5.6(2)	12.6(4)
	0.0235	4.0(2)	10.5(4)

<sup>a</sup>  $\Delta_{M-C}$  = the difference in bond lengths of the metal to C(11) and C(15) bonds and the metal to C(12), C(13), and C(14) bonds. <sup>b</sup> HA = angle between planes [C(12), C(13), C(14)] and [C(12), C(11), C(15), C(16)]. <sup>c</sup> FA = angle between planes [C(12), C(11), C(15), C(16)] and [C(19), C(11), C(15), C(16)].

carbon bond lengths of the noncoordinated arene ring, reflecting a partially localized cyclohexatriene structure.<sup>27</sup> Slipped  $\eta^3$ -coordinated complexes<sup>26</sup> will possess nearly equal carbon–carbon bond lengths in the arene ring, as observed in fully delocalized benzene itself. The arene ring carbon–carbon bond lengths in the indenyl ligands in complexes **4a**, **4b**, and **4b'** are tabulated in Table 6. Taken together, the indenyl structural data indicate that one of the ancillary ligands in complex **4b'**

(29) In several specific examples, the authors do not report HA values.<sup>27a,c</sup>



**Table 6. Internal Carbon–Carbon Indenyl Bond Lengths (Å)**

	C(11)–C(12)	C(12)–C(13)	C(13)–C(14)	C(14)–C(15)	C(11)–C(15)	C(15)–C(16)	C(16)–C(17)	C(17)–C(18)	C(18)–C(19)	C(19)–C(11)
<b>4a</b>	1.438(9)	1.413(10)	1.404(9)	1.406(9)	1.431(9)	1.423(9)	1.362(10)	1.406(11)	1.314(10)	1.414(9)
	1.430(8)	1.397(8)	1.430(8)	1.437(8)	1.428(8)	1.419(8)	1.366(9)	1.405(9)	1.361(8)	1.399(8)
<b>4b</b>	1.419(3)	1.416(3)	1.406(3)	1.415(3)	1.426(3)	1.423(4)	1.352(4)	1.404(4)	1.347(4)	1.413(3)
	1.442(9)	1.405(8)	1.405(13)	1.425(15)	1.440(11)	1.37(2)	1.45(3)	1.410(19)	1.356(6)	1.419(5)
<b>4b'</b>	1.438(10)	1.429(10)	1.380(9)	1.423(8)	1.433(7)	1.417(8)	1.378(12)	1.445(14)	1.367(6)	1.397(4)
<b>3a</b>	1.439(8)	1.401(8)	1.427(8)	1.435(8)	1.418(8)	1.429(8)	1.374(8)	1.397(9)	1.343(9)	1.424(8)
	1.433(8)	1.418(8)	1.417(8)	1.423(8)	1.432(8)	1.401(8)	1.378(9)	1.383(10)	1.361(10)	1.419(8)
<b>7</b>	1.417(3)	1.422(3)	1.418(3)	1.428(3)	1.428(3)	1.416(3)	1.365(4)	1.413(4)	1.364(4)	1.419(3)
	1.425(3)	1.424(3)	1.409(3)	1.431(3)	1.427(4)	1.416(3)	1.370(4)	1.401(5)	1.365(4)	1.414(4)
<b>8</b>	1.436(4)	1.414(4)	1.423(4)	1.427(4)	1.422(4)	1.433(4)	1.360(4)	1.415(4)	1.371(4)	1.418(4)
	1.425(4)	1.416(4)	1.427(4)	1.430(4)	1.432(4)	1.426(4)	1.364(4)	1.409(4)	1.365(4)	1.412(4)

**Table 7. Structural Data for Amino Substituent**

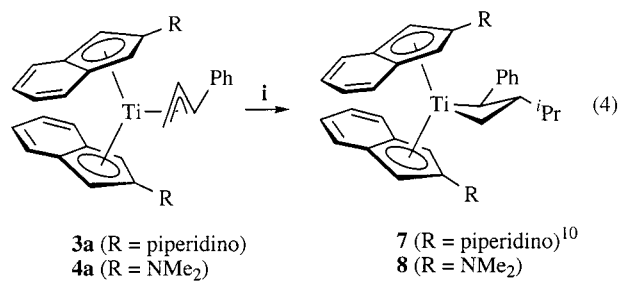
complex	pyramidalization (%)	C <sub>Ind</sub> –N (Å)	twist angle (deg)
<b>3a</b>	51	1.416(7)	7.1
	74	1.409(7)	28.3
<b>4a</b>	28	1.399(9)	21.4
	43	1.382(8)	16.9
<b>4b</b>	32	1.396(3)	17.1
	34	1.407(6)	–158.8
<b>4b'</b>	32	1.396(3)	7.0
	30	1.408(13)	4.8
<b>7</b>	43	1.397(3)	6.4
	54	1.399(3)	8.6
<b>8</b>	3	1.366(4)	–171.4
	22	1.375(4)	5.8

is “distorted” toward  $\eta^3$ -coordination, while the remaining indenyl rings show relatively unperturbed  $\eta^5$ -coordination. The lower accuracy of the structural determination for complex **4b/4b'**, however, clearly suggests caution in interpreting this apparent ring slippage.

The geometry and rotational orientation of the amino substituents on the indenyl rings were also determined. For the greatest donation of electron density from the ancillary ligands to the metal, the lone pair on the nitrogen atom ideally aligns parallel to the  $\pi$ -system of the cyclopentadienyl ring and the hybridization of the nitrogen atom approaches  $sp^2$ . The degree of pyramidalization,<sup>30</sup> the twist angle between the axis of the lone electron pair on nitrogen and the  $\pi$ -electron system of the indenyl ring,<sup>31</sup> and the indenyl carbon–nitrogen bond lengths together indicate the extent of electron donation from the amino group into the indenyl ring. These values have been determined for complexes **3a**, **4a**, and **4b** and are collected in Table 7. The amino groups in all of these complexes are significantly pyramidal, deviate markedly from coplanarity with the indenyl ring, and possess C<sub>Ind</sub>–N bond lengths only minimally contracted from normal C–N single bonds. The structural and orientational parameters of the ancillary ligands in cinnamyl complexes **3a** and **4a** are surprisingly similar.

**Syntheses of Titanacyclobutane Complexes 7, 8, and 9.** Both 3-isopropyl-2-phenylbis(2-piperidinoindenyl)titanacyclobutane (**7**)<sup>10</sup> and 3-isopropyl-2-phenylbis(2-*N,N*-dimethylaminoindenyl)titanacyclobutane (**8**) can be synthesized from the Ti(III) cinnamyl precursors **3a** and **4a**, respectively, upon addition of 1 equiv each of isopropyl iodide and samarium diiodide<sup>32,33</sup> at low

temperature<sup>34</sup> (eq 4). Thermally stable and deep red in



Conditions: i. *i*-PrI, SmI<sub>2</sub>, –35 °C → RT, THF, 14h; **7**: 78%; **8**: 84%.

color, complex **8** is isolated by evaporation of the solvent and extraction into a mixture of benzene and hexane (1:2). Suitable crystals for X-ray diffraction were obtained from THF layered with hexane and cooled to –35 °C. Under similar conditions, single crystals of the previously reported complex **7** were obtained from diethyl ether layered with pentane.

Spectroscopic analysis reveals that complex **8** is fluxional at room temperature: warming the complex in solution (70 °C) results in the sharpening of the two broad indenyl singlets observed at  $\delta$  4.27 and 4.05 into mutually coupled doublets with a coupling constant of 2.1 Hz. Once this fast exchange limit is reached, the featureless titanacyclobutane  $\alpha$ -CH<sub>2</sub> signal sharpens into a triplet with a coupling constant of 9.6 Hz. The complex exhibits NMR spectra completely consistent with previously reported disubstituted titanacyclobutanes,<sup>7,10</sup> including characteristic upfield resonances for the  $\beta$ -hydrogen atom and one of the two  $\alpha$ -methylene hydrogen atoms.

Because the isolation of crotyltitanium(III) complex **4b** proved to be difficult, a one-pot alkylation procedure was used to obtain crotyl-derived titanacyclobutane complexes without the isolation of this intermediate. Thus, chloride complex **5** was alkylated in situ with crotyl Grignard, followed by addition of 1 equiv each of isopropyl iodide and SmI<sub>2</sub>, providing titanacyclobutane complex **9** as dark purple microcrystals in 68% yield (eq

(30) Percent pyramidalization =  $[360 - \sum \text{carbon–nitrogen bonds}] / [360 - 328.5] \times 100$ .

(31) The twist angle is the angle the lone pair on the nitrogen atom makes with the [C12–C13–C14] (or [C22–C23–C24]) plane, that is, the plane of the indenyl  $\pi$ -system.

(32) Casty, G. L.; Stryker, J. M. *J. Am. Chem. Soc.* **1995**, *117*, 7814.

(33) Girard, P.; Namy, J. L.; Kagan, H. B. *J. Am. Chem. Soc.* **1980**, *102*, 2693.

(34) The short reaction time and low temperature conditions for the central carbon alkylation contrast the elevated temperatures required for the reaction of secondary alkyl iodides with samarium iodide<sup>33</sup> and for the samarium-mediated alkylation of (C<sub>5</sub>Me<sub>5</sub>)<sub>2</sub>Ti( $\eta^3$ -allyl) with isopropyl iodide.<sup>32</sup> We suspect that under our reaction conditions, SmI<sub>2</sub> itself is not responsible for initial radical generation. Instead, we believe that the electron-rich Ti(III) complexes **3a** and **4a** react directly with the haloalkane, leading to the formation of an allyltitanium(IV) halide intermediate and the isopropyl radical, the latter of which alkylates the remaining Ti(III) allyl complex. The allyltitanium(IV) halide intermediate is then reduced by SmI<sub>2</sub> to regenerate the allyltitanium(III) complex, as proposed for related propargyltitanium(III) alkylations.<sup>1b</sup>

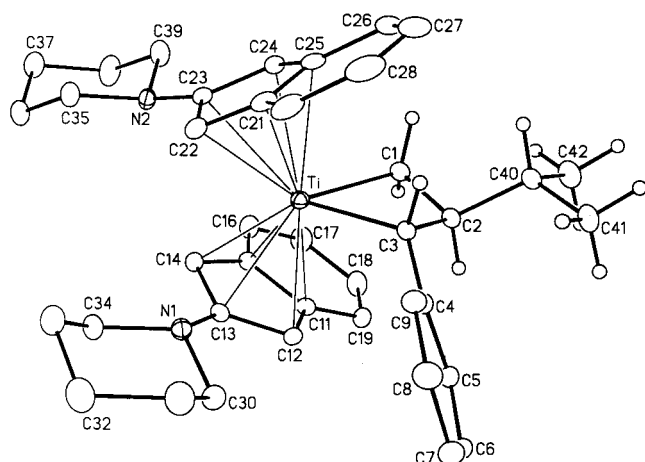


**Figure 7.** Molecular structure of **7**. Selected interatomic distances and angles are listed in Table 8.

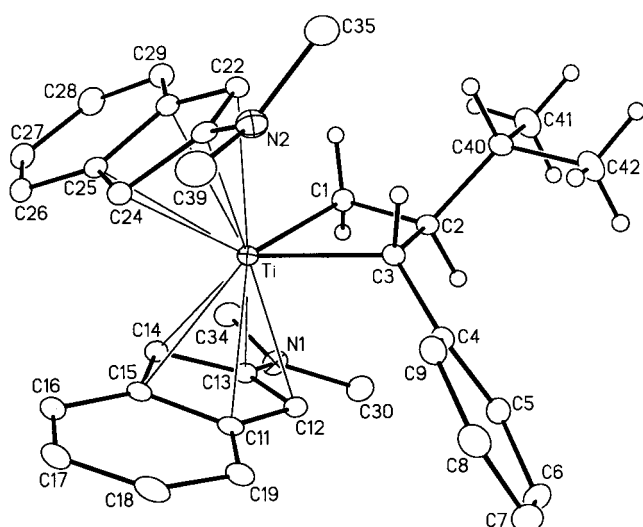
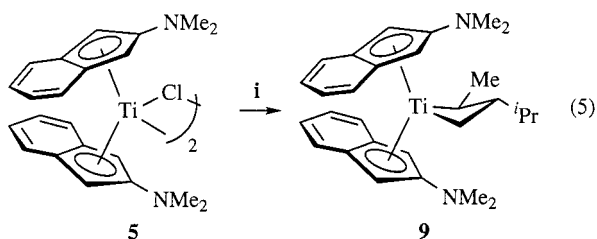


**Figure 8.** Molecular structure of **8**. Selected interatomic distances and angles are listed in Table 9.

5). In contrast to the thermally unstable crotyl-derived



Conditions: i.  $\text{CH}_3\text{CH}=\text{CHCH}_2\text{MgCl}$ ,  $-35\text{ }^\circ\text{C}\rightarrow\text{RT}$ , THF, 1h; then  $^i\text{PrLi}$ ,  $\text{Sml}_2$ ,  $-35\text{ }^\circ\text{C}\rightarrow\text{RT}$ , THF, 0.5h; 66%.

titanacyclobutane complexes obtained from the bis(2-*pi*-peridinoindenyl) complex **3b**,<sup>10</sup> the bis(2-*N,N*-dimethylaminoindenyl)titanacyclobutane **9** is substantially more stable; notable decomposition is observed only after several hours in solution at room temperature.

**Solid-State Structures of Titanacyclobutane Complexes 7 and 8.** ORTEP diagrams of complexes **7** and **8**, together with the atomic labeling schemes, are shown in Figures 7 and 8, respectively. Selected intramolecular bond lengths and angles are presented in Tables 8 and 9. Homonuclear decoupling experiments, difference NOE measurements, and  $^1\text{H}$ - $^{13}\text{C}$  hetero-

**Table 8.** Selected Bond Lengths (Å) and Angles (deg) for Complex **7**

Ti-C1	2.121(2)	N1-C13	1.397(3)
Ti-C3	2.190(2)	N1-C30	1.453(3)
Ti-C11	2.497(2)	N1-C34	1.466(3)
Ti-C12	2.418(3)	N2-C23	1.399(3)
Ti-C13	2.420(2)	N2-C35	1.463(3)
Ti-C14	2.367(2)	N2-C39	1.465(3)
Ti-C15	2.437(2)	C1-C2	1.553(3)
Ti-C21	2.479(3)	C2-C3	1.552(3)
Ti-C22	2.393(3)	Ti-Cp(cent) <sup>a</sup>	2.105, 2.158
Ti-C23	2.529(3)	Ti-Cp(plane) <sup>b</sup>	2.1029(12), 2.1569(12)
Ti-C24	2.460(3)		
Ti-C25	2.505(3)		

C1-Ti-C3	71.33(9)	C13-N1-C30	117.1(2)
C1-C2-C3	108.09(19)	C13-N1-C34	116.5(2)
Cp(cent)-M-Cp(cent) <sup>a</sup>	131.3	C30-N1-C34	112.9(2)
Cp(plane)-M-Cp(plane) <sup>b</sup>	52.03(11)	C23-N2-C35	114.4(2)
		C23-N2-C39	116.07(19)
		C35-N2-C39	112.4(2)

<sup>a</sup> Centroid of the indenyl ligand. <sup>b</sup> Calculated normal to plane of indenyl ligand.

**Table 9.** Selected Bond Lengths (Å) and Angles (deg) for Complex **8**

Ti-C1	2.128(3)	N1-C13	1.366(4)
Ti-C3	2.202(2)	N1-C30	1.450(4)
Ti-C11	2.439(3)	N1-C34	1.448(4)
Ti-C12	2.401(3)	N2-C23	1.375(4)
Ti-C13	2.516(3)	N2-C35	1.452(4)
Ti-C14	2.381(3)	N2-C39	1.442(4)
Ti-C15	2.462(3)	C1-C2	1.559(4)
Ti-C21	2.463(3)	C2-C3	1.557(4)
Ti-C22	2.423(3)	Ti-Cp(cent) <sup>a</sup>	2.104, 2.117
Ti-C23	2.504(3)	Ti-Cp(plane) <sup>b</sup>	2.099(3), 2.116(3)
Ti-C24	2.387(3)		
Ti-C25	2.460(3)		

C1-Ti-C3	71.84(10)	C13-N1-C30	120.0(2)
C1-C2-C3	109.3(2)	C13-N1-C34	120.0(2)
Cp(cent)-M-Cp(cent) <sup>a</sup>	133.1	C30-N1-C34	119.0(2)
Cp(plane)-M-Cp(plane) <sup>b</sup>	49.8(3)	C23-N2-C35	116.9(2)
		C23-N2-C39	118.6(2)
		C35-N2-C39	117.6(3)

<sup>a</sup> Centroid of the indenyl ligand. <sup>b</sup> Calculated normal to plane of indenyl ligand.

nuclear correlated spectroscopy were used to determine the structure of complex **7** in solution, supporting a tentative assignment of the substituent stereochemistry as *trans*.<sup>10</sup> Crystallography confirms the spectroscopic characterization of both titanacyclobutane complexes **7** and **8**.

In complexes **7** and **8**, the Ti-C(1) and Ti-C(3) bond distances, respectively, are essentially equidistant and fall close to the statistical range for previously determined Ti-C<sub>sp</sub><sup>3</sup> bonds (2.14–2.21 Å).<sup>35</sup> The unsubstituted Ti-C(1) bonds are consistently shorter than Ti-C(3), presumably due to the absence of a substituent and the inherently weaker bonding to a benzylic position. The carbon-carbon bond lengths in the titanacyclobutane rings are roughly equal in length and comparable to previously characterized titanacyclobutane complexes.<sup>36</sup> The metallacycle rings are puckered, with dihedral

(35) Orpen, A. G.; Brammer, L.; Allen, F. H.; Kennard, O.; Watson, D. G.; Taylor, R. *J. Chem. Soc., Dalton Trans.* **1989**, S1.

(36) (a) Lee, J. B.; Gajda, G. J.; Schaefer, W. P.; Howard, T. R.; Ikariya, T.; Straus, D. A.; Grubbs, R. H. *J. Am. Chem. Soc.* **1981**, *103*, 7358. (b) Stille, R. J.; Santarsiero, B. D.; Grubbs, R. H. *J. Org. Chem.* **1990**, *55*, 843. (c) Polse, J. L.; Anderson, R. A.; Bergman, R. G. *J. Am. Chem. Soc.* **1996**, *118*, 8737. (d) Polse, J. L.; Kaplan, A. W.; Anderson, R. A.; Bergman, R. G. *J. Am. Chem. Soc.* **1998**, *120*, 6316.

angles of 157.0° and 156.5° for the C(1)–Ti–C(3) and C(1)–C(2)–C(3) planes of complexes **7** and **8**, respectively. Such puckering is typical of  $\alpha,\beta$ -disubstituted titanacyclobutane complexes.<sup>36b–d</sup> The ancillary ligands are positioned with indenyl rotational angles of 106.9° and 124.0°, respectively. In titanacyclobutane **7**, however, the arene ring of one piperidinoindenyl ligand flanks each side of the metallacycle fragment, while in complex **8** the dimethylamino groups flank each side of the titanacyclobutane core, presumably a consequence of the lower steric demand of the dimethylamino substituents.

The increase in oxidation state to titanium(IV) upon alkylation is clearly reflected in accompanying changes in nitrogen pyramidalization, C<sub>Ind</sub>–N bond length, and tilt angle of the amino substituents, as compared to the Ti(III) precursors. The amine functionality on each indenyl ring is significantly less pyramidal (Table 7), the C<sub>Ind</sub>–N bond length is shorter, and the tilt angle is smaller, all indicative of the stronger donation of electron density into the indenyl ligands for the higher oxidation state products. The slip parameters, hinge and fold angles, and carbon–carbon bond lengths for each of the indenyl rings (Tables 5 and 6) suggest mildly distorted  $\eta^5$ -coordination, but show no systematic correlation with the change in oxidation state.

## Discussion

**Titanium(III) Complexes.** The bis(2-*N,N*-dimethylaminoindenyl)titanium(III) template affords improved results for regioselective central carbon radical alkylation of substituted allyl complexes relative to the previously reported bis(2-piperidinoindenyl)titanium(III) template.<sup>10</sup> Central carbon alkylation proceeds in acceptable yields upon reaction with both stabilized and unstabilized radicals.<sup>11</sup> Titanacyclobutane complexes derived from crotyl complex **4b**, which possesses  $\beta$ -hydrogen atoms on the titanacyclobutane  $\alpha$ -substituent, are found to have reasonable thermal stability. Preliminary investigation into both carbon monoxide and isonitrile insertion suggests the development of a general synthesis of organic 2,3-disubstituted cyclobutanones<sup>3</sup> and cyclobutanamines,<sup>2</sup> respectively. These results, together with the unusual structural features reported for the crystal structure of complex **3a** (Figure 3),<sup>10</sup> prompted this extended structural investigation.

In the synthesis of bis(2-*N,N*-dimethylaminoindenyl)titanium chloride **5**, the complex is initially formed as the solvated lithium chloride adduct, **5**·LiCl(THF)<sub>2</sub>. Under high vacuum, the THF is lost and lithium chloride is released from the coordination sphere. The solid-state structure of complex **5** remains ambiguous: the complex could not be obtained as single crystals. Tentatively, we assign the structure as a chloride-bridged dimer, a consequence of the intermediate steric demand of the ancillary ligand.<sup>22</sup> The crystal structure of complex **5**·LiCl(THF)<sub>2</sub> possesses a crystallographic 2-fold rotational axis passing through the titanium and lithium atoms. The planar MCl<sub>2</sub>–Li core, rare in the chemistry of titanium(III) halides,<sup>37</sup> possesses a Ti–Cl distance elongated with respect to the statistical range determined for Ti(IV)–Cl bond lengths (2.442–2.476 Å)<sup>35</sup> and shortened with respect to reported Ti(III)–Cl

bond lengths (2.527–2.555 Å).<sup>35</sup> The ancillary ligands in complex **5**·LiCl(THF)<sub>2</sub> are positioned with an indenyl rotational angle of 129.6°, where the dimethylamino groups flank each side of the TiCl<sub>2</sub>Li core. More interestingly, the nitrogen pyramidalization (14.8%), C<sub>Ind</sub>–N bond length, and tilt angle (11.8°) of the amino substituents are intermediate between the values determined for Ti(III) complexes **4a** and **4b** and Ti(IV) complex **8**.

In an attempt to identify potential structural origins for the differences in reactivity identified for the two aminoindenyl ligand systems, crystal structures were determined for the two 2-*N,N*-dimethylaminoindenyl Ti(III) complexes **4a** and **4b**, allowing for direct comparisons with the structurally characterized 2-piperidinoindenyl derivative **3a**. In the case of the cinnamyl complexes **3a** and **4a**, striking similarities in the general appearance are evident. Upon close inspection, however, many subtle structural differences are noted. In the coordination of the cinnamyl ligand, the phenyl-substituted Ti–C(3) bond is longer in 2-*N,N*-dimethylaminoindenyl complex **4a** compared to 2-piperidinoindenyl complex **3a**, while the C(3)–C(4) bond is longer in complex **3a** than in complex **4a** (Table 4). One interpretation of these data is that in complex **3a** the substituted allyl ligand is distorted toward  $\eta^1,\eta^2-(\sigma,\pi)$ -coordination, imbuing the benzylic carbon with somewhat greater  $\sigma$ -character. The C(1)–C(2) bond consequently acquires greater  $\pi$ -character, consistent with the shorter bond length observed in this complex. As a result, the phenyl group is thus expected to be less conjugated to the allyl framework; this is reflected directly in the longer C(3)–C(4) bond. While it is counterintuitive that the more sterically crowded complex **3a** displays the shorter benzylic carbon–titanium bond, the more symmetrical  $\pi$ -allyl structure defined for the 2-*N,N*-dimethylaminoindenyl complex **4a** correlates with a more selective reactivity toward organic radicals. It is, however, also plausible that (intermolecular) crystal packing forces in the extended lattices alone account for the observed differences in cinnamyl ligand coordination.

The difference in nitrogen parameters between piperidinoindenyl complex **3a** and *N,N*-dimethylaminoindenyl complex **4a** is suggestive of varying electron richness at the metal center, although the effects of crystal packing forces on these parameters also cannot be disregarded. While the differences in twist angle are ambiguous, the amino substituents in complex **3a** show greater pyramidalization and longer C<sub>Ind</sub>–N bond lengths than observed in complex **4a**, implying that the slightly more electron rich piperidinoindenyl ligands in complex **3a** provide less electron density to the metal than do the *N,N*-dimethylaminoindenyl ligands in complex **4a** (Table 7). The exaggerated pyramidal character observed in the piperidino nitrogen atoms may simply reflect geometric constraints inherent to the cyclic substituent, which resist the expansion of the C–N–C bond angle that must accompany deformation toward trigonal (sp<sup>2</sup>) nitrogen.

(37) To our knowledge, only two examples of complexes possessing the Ti(Cl)<sub>2</sub>Li core have been previously characterized: Dick, D. G.; Duchateau, R.; Edema, J. J. H.; Gaborratta, S. *Inorg. Chem.* **1993**, *32*, 1959. Scoles, L.; Minhas, R.; Duchateau, R.; Jubb, J.; Gambarotta, S. *Organometallics* **1994**, *13*, 4978.

Although the slip parameters, hinge angles, and fold angles do not indicate significant ring slip in the ancillary ligands of complexes **3a** and **4a**, close examination of bond alternation for the internal carbon–carbon bond lengths of the benzene ring (Table 6) suggests a greater retention of the arene aromaticity in piperidinoindenyl complex **3a**. The *N,N*-dimethylaminoindenyl ancillary ligands in complex **4a** show a pattern more consistent with an  $\eta^5$ -cyclopentadienyl bonding, as evidenced by the statistically significant bond length alternation in the internal carbon–carbon bond lengths of the arene rings. While this also suggests that greater electron density is delivered to the metal in *N,N*-dimethylaminoindenyl complex **4a**, the extent to which these differences affect the reactivity of the two titanocene templates remains unclear. What is clear, however, is that in all of the Ti(III) complexes, the amine functionality is capable of providing far greater donation of electron density to the ligand system than is required by the metal and, as a result, the system at least partially “deconjugates” the nitrogen center.<sup>38</sup>

Among the structurally characterized Ti(III) allyl complexes,<sup>23</sup> crotyl complexes **4b** and **4b'** display the shortest Ti–C1 and Ti–C2 bonds reported, reflecting relatively strong  $d \rightarrow \pi^*$  back-donation from the  $d^1$ -metal center. Despite the lower quality of the structure determination, the coordination of the crotyl ligands clearly differs significantly between conformational isomers **4b** and **4b'**. Analogous to the distortions identified in complex **3a**, the allyl ligand in conformer **4b** appears to be distorted toward  $\eta^1, \eta^2$ -( $\sigma, \pi$ )-coordination, whereas in conformer **4b'**, the allyl coordination is more symmetrical. These differences among “identical” molecules clearly illustrate that considerable coordinative freedom exists in this series and underscore the importance of crystal packing forces in determining structural detail.

More interestingly, conformational isomers **4b** and **4b'** differ markedly in ancillary ligand coordination, particularly with respect to deviations from idealized  $\eta^5$ -coordination. While the  $\Delta_{M-C}$  value of 0.1437 Å for conformer **4b'** is not complemented by a significant hinge angle, the data reveal that the unique indenyl ligand displays longer Ti–C bonds to the ring junction carbons relative to the remaining Ti–C bonds in the five-membered ring. This distortion toward  $\eta^3$ -coordination is not observed for either of the indenyl ligands in conformer **4b**, which show stronger coordination to the ring junction carbons and hinge angles reflective of the longer bonds observed to the dimethylamino-substituted ring carbons. In complex **4b'**, both the extent of pyramidalization and  $C_{Ind-N}$  bond lengths are consistent with those observed in complexes **4a**, **4b**, and **3a**, but the alignment of the nitrogen lone pair with the indenyl  $\pi$ -system is nearly perfect. The resultant increase in electron donation may compensate for the loss in electron density arising from the “slipped” coordination of one indenyl ligand; this in turn may give rise to the differences in crotyl coordination noted between the conformational isomers **4b** and **4b'**.

(38) Amine substituents on coordinated cyclopentadienyl rings are known to provide variable amounts of electron density to the metal center, depending on the electronic state of the metal. Carbon–nitrogen bond lengths in  $\eta^5$ -aminocyclopentadienyl complexes are longer in electron-rich organometallic systems (e.g., ferrocenes, ca. 1.41 Å)<sup>41c,e</sup> and shorter when coordinated to electron-deficient organometallic fragments (e.g.,  $Mn(CO)_3$  in cymantrenes, ca. 1.36 Å).<sup>40d</sup>

**Titanacyclobutane Complexes.** Regioselective, central carbon radical alkylation of allyltitanium(III) complexes **3a**, **4a**, and **4b** provides *trans*-2,3-disubstituted titanacyclobutane complexes in reasonable yields. Crystallographic analysis of titanacyclobutane complexes **7** and **8** reveal core structures very similar to previously reported 2,3-disubstituted titanacyclobutane complexes.<sup>36</sup> ORTEP diagrams (Figure 6 and 7) depict the anticipated *trans* stereochemistry and significant ring puckering. The H–H torsion angle for H–C(2)–C(3)–H in complex **7** is calculated to be 155.6°, corresponding to a coupling constant of approximately 10 Hz based on the Karplus relation.<sup>39</sup> This prediction is in good agreement with the 11.6 Hz coupling observed in the <sup>1</sup>H NMR spectrum, suggesting that the solution structure is reasonably modeled by the solid-state structure. For titanacyclobutane complex **8**, the H–H torsion angle for H–C(2)–C(3)–H is 147.3°, again in good agreement with the 10.7 Hz coupling observed in the <sup>1</sup>H NMR spectrum. The principal difference in the solid-state structures of the complexes **7** and **8** lies in the relative orientation of the ancillary ligands. The increased steric demand of the larger piperidine substituents in complex **7** presumably forces the indenyl rings to rotate, placing the substituents behind the titanocene wedge. In contrast, the dimethylamino substituents in complex **8** project somewhat forward over the titanacyclobutane ring. It is not obvious, however, that such a conformational shift would necessarily be observed in the corresponding crotyl-derived titanacyclobutane complexes and how, if observed, such a change might engender the observed difference in the relative rates of  $\beta$ -hydride elimination.

The change in oxidation state at the metal that accompanies central carbon alkylation is accentuated by rehybridization of the nitrogen atoms and rotation of the amine functionality with respect to the indenyl plane. Compared to the respective Ti(III) precursors, the amino substituents in complexes **7** and **8** are significantly less pyramidal and show shorter  $C_{Ind-N}$  bond lengths. In addition, the tilt angle between the lone pair on nitrogen and the  $\pi$ -system of the indenyl fragment is greatly reduced relative to the Ti(III) complexes. The greater ability of the nitrogen-substituted ancillary ligand system to facilitate the oxidation state increase at the metal in the transition state for central carbon alkylation may, at least in part, account for the successful alkylation of substituted allyl complexes.

Although the piperidinoindenyl ligands in complex **7** indeed reflect the change in oxidation state relative to complex **3a**, the nitrogen pyramidalization is greater and the  $C_{Ind-N}$  bond lengths are longer than that observed in either 1,1'-bis(2-*N,N*-dimethylamino)titanocene dichloride<sup>40a</sup> or any of the previously reported bis(dialkylamino)zirconocene dichlorides.<sup>40d,f,g,i</sup> Only *ansa*-bridged bis(dialkylaminoindenyl)zirconium(IV) systems exhibit nitrogen pyramidalizations and  $C_{Ind-N}$  bond lengths that approach the values present in complex **7**, although in the *ansa*-bridged systems these features are attributed to specific steric interactions with the ligand bridges.<sup>40g,h</sup>

In contrast, the crystal structure of *N,N*-dimethylaminoindenyl complex **8** reveals that the amine func-

(39) Silverstein, R. M.; Webster, F. X. *Spectroscopic Identification of Organic Compounds*, 6th ed.; John Wiley & Sons: New York, 1998.

tionality is essentially  $sp^2$ -hybridized. The observed  $C_{\text{Ind}}\text{--N}$  bond lengths indicate strong double bond character (cf., imine  $C=N$ : 1.38 Å) and fall within the range observed for other dialkylaminoindenyl complexes of Ti(IV) and Zr(IV).<sup>40</sup> The twist angle is similarly decreased, confirming the strong donation of electron density into the indenyl rings. While the differences in structural parameters observed for the aminoindenyl ligands in complexes **7** and **8** are indeed pronounced, such differences cannot be readily rationalized by simple steric and electronic considerations.

### Conclusions

The ORTEP diagrams of Ti(III) and Ti(IV) complexes **3a**, **4a**, **4b**, **5**·LiCl(THF)<sub>2</sub>, **7**, and **8** reveal interesting

(40) (a) Stahl, K. P.; Boche, G.; Massa, W. *J. Organomet. Chem.* **1984**, *277*, 113. (b) Bernheim, M.; Boche, G. *Angew. Chem., Int. Ed. Engl.* **1990**, *19*, 1010. (c) Plenio, H.; Burth, D. *Angew. Chem., Int. Ed. Engl.* **1995**, *34*, 800. (d) Plenio, H.; Burth, D. *Organometallics* **1996**, *15*, 1151. (e) Plenio, H.; Burth, D. *Organometallics* **1996**, *15*, 4054. (f) Plenio, H.; Burth, D. *J. Organomet. Chem.* **1996**, *519*, 269. (g) Barsties, E.; Schaible, S.; Proscenc, M.-H.; Rief, U.; Röhl W.; Weyand, O.; Dorer, B.; Brintzinger, H.-H. *J. Organomet. Chem.* **1996**, *520*, 63. (h) Luttkhedde, H. J. G.; Leino, R.; Ahlgrén, M. J.; Pakkanen, T. A.; Näsman, J. H. *J. Organomet. Chem.* **1998**, *557*, 227. (i) Knüppel, S.; Fauré, J.-L.; Erker, G.; Kehr, G.; Nissenen, M.; Fröhlich, R. *Organometallics* **2000**, *19*, 1262.

structural features presumably attributable to the variable electron demands of titanium centers in the different ligand and oxidation state environments. The crystal structures clearly indicate that the ancillary ligands are capable of providing greater electron density than is required by the metal, facilitating the oxidation state change that occurs during central carbon radical alkylation. Based on this “oversupply” of electron richness, current investigations are focused on the development of less electron rich templates, to determine the minimum electron density required to promote regioselective central carbon alkylation of substituted allyl systems.

**Acknowledgment.** Financial support from Natural Sciences and Engineering Research Council of Canada and the University of Alberta is gratefully acknowledged.

**Supporting Information Available:** ORTEP diagrams and tables of crystal, data collection, and refinement parameters, atomic coordinates, bond distances and angles, and isotropic displacement parameters for complexes **4a**, **4b**, **5**, **7**, and **8**. This material is available free of charge via the Internet at <http://pubs.acs.org>.

OM000799N